

I

A STRUCTURAL INVESTIGATION OF  
THE MERCURY - TIN SYSTEM

II

THE DETERMINATION OF THE  
CRYSTAL STRUCTURE OF THE SIGMA  
PHASE BY APPLICATION OF X-RAY  
DIFFRACTION METHODS TO THIS  
PHASE IN THE IRON - CHROMIUM AND  
IRON - MOLYBDENUM SYSTEMS

Thesis by

B. Gunnar Bergman

In Partial Fulfillment of the Requirements

for the Degree of

Doctor of Philosophy

California Institute of Technology

Pasadena, California

1951

## ACKNOWLEDGEMENT

During my research work for this thesis and also during the preparation of it I have received valuable assistance and advice from many persons which I have acknowledged elsewhere in this thesis. I am, however, particularly much indebted to Professor Linus Pauling for suggesting this research work, for his interest in my work and for his valuable advice, and to Dr. David P. Shoemaker whose contribution in <sup>the</sup> form of valuable advice and criticism, interest in my work and encouragement has been of <sup>the</sup> greatest importance for the rapid and successful conclusion of it. I want to use the opportunity to express my thanks to these two persons.



ABSTRACT

A study of the mercury-tin system has been made by the application of thermal analysis and x-ray powder methods in order to determine whether four hypothetical intermetallic compounds of the compositions  $\text{HgSn}_{35}$ ,  $\text{HgSn}_{17}$ ,  $\text{HgSn}_{11}$  and  $\text{HgSn}_8$  proposed by Professor Linus Pauling, exist. The thermal analysis did not indicate the presence of these compounds in equilibrium with the liquid phase. By x-ray powder methods the occurrence of only two different phases was established, one of tetragonal structure and identical with that of white tin, and one of simple hexagonal structure as has been reported by previous workers. The four intermetallic compounds proposed by Professor Pauling do not seem to exist.

The structure of the sigma phase in the iron-chromium system at 46.5 at. % chromium content has been successfully determined by the application of x-ray diffraction methods. The structure is of a type that has not been observed earlier in intermetallic compounds.

The structure of the sigma phase in the iron-molybdenum system has also been investigated briefly and found to be of the same type as the iron-chromium sigma structure.

## TABLE OF CONTENTS

<u>PART</u>	<u>TITLE</u>	<u>PAGE</u>
I.	A STRUCTURAL INVESTIGATION OF THE MERCURY-TIN SYSTEM . . . . .	1
	Introduction . . . . .	1
	Previous work . . . . .	4
	Experimental . . . . .	6
	Thermal analysis . . . . .	6
	X-ray analysis . . . . .	7
	Discussion . . . . .	13
	Acknowledgement . . . . .	14
	Summary . . . . .	14
	References . . . . .	16
II.	THE DETERMINATION OF THE CRYSTAL STRUCTURE OF THE SIGMA PHASE BY THE APPLICATION OF X-RAY DIFFRACTION METHODS TO THIS PHASE IN THE IRON-CHROMIUM AND IRON-MOLYBDENUM SYSTEMS . . . . .	17
	Introduction . . . . .	17
	Experimental . . . . .	24
	Materials . . . . .	24
	Preliminary powder work . . . . .	24
	The search for single crystals . . . . .	25
	Description of the single crystals . . . . .	26
	The Laue symmetry of the sigma phase crystal structure . . . . .	27
	The approximate determination of unit cell dimensions . . . . .	28
	The refinement of the unit cell dimensions . . . . .	31
	The derivation of a tentative structure and the possible space groups . . . . .	38

TABLE OF CONTENTS (continued)

<u>PART</u>	<u>TITLE</u>	<u>PAGE</u>
II.	The testing of the tentative structure . . .	47
	The final determination of the space group .	54
	The refinement of the tentative structure. .	56
	General aspects . . . . .	56
	The collection of intensity data . . . .	57
	Estimation of intensities . . . . .	57
	Calculations . . . . .	59
	The results of the refinement of para- meters . . . . .	67
	Discussion of the structure . . . . .	75
	General remarks . . . . .	75
	The coordination polyhedra and inter- atomic distances . . . . .	75
	The possible ordering of the iron and chromium atoms . . . . .	78
	Brillouin zone stabilization . . . . .	85
	Work on the iron-molybdenum sigma phase structure . . . . .	87
	Introduction . . . . .	87
	Materials . . . . .	87
	Single crystal work . . . . .	88
	Powder work . . . . .	88
	Discussion . . . . .	89
	Summary . . . . .	90
	Acknowledgements . . . . .	92
	References . . . . .	93
	Propositions . . . . .	95
	References . . . . .	98

PART I

A STRUCTURAL INVESTIGATION OF THE MERCURY-TIN SYSTEM

INTRODUCTION

In a memorandum to Dr. David P. Shoemaker, dated August 22, 1949, Professor Linus Pauling suggested that the tin-rich side of the tin-mercury system might contain compounds with the formulae  $\text{HgSn}_{35}$ ,  $\text{HgSn}_{17}$ ,  $\text{HgSn}_{11}$ ,  $\text{HgSn}_8$ . On the basis of work which indicated that tin containing a little mercury crystallizes in a basic structure having one atom at each point of a<sup>a</sup> hexagonal lattice, Professor Pauling arrived at these formulae in the following way:

Consider a hexagonal cell with  $a' = 6a_0$  and  $c' = 3c_0$  where  $a_0$  and  $c_0$  are the lattice constants for the simple hexagonal sublattice. This larger cell contains 108 sublattice points. To obtain the  $\text{HgSn}_{35}$  structure, place Hg-atoms at (000) and corresponding rhombohedral lattice positions of the larger cell ( $2/3 \ 1/3 \ 1/3$ ) and ( $1/3 \ 2/3 \ 2/3$ ) and tin at all other sublattice points as shown in Figure 1. Eight of the thirty-five tin atoms surround the mercury atom in the first coordination polyhedron (a hexagonal bipyramid). Twenty-four tin atoms are in the second coordination polyhedron (12 in the equatorial plane, 6 above, and 6 below). Finally there are 3 extra tin atoms in the basal plane with positions ( $1/2 \ 0 \ 0$ ), ( $1/2 \ 1/2 \ 0$ ) and ( $0 \ 1/2 \ 0$ ),

and 3 extra tin atoms in corresponding positions in each of the other two layers in the large cell, adding up to a total of 9 extra atoms in the large unit. By substituting mercury atoms for three of these extra tin atoms (one in each sublattice layer), we get an orthorhombic structure of the composition  $\text{HgSn}_{17}$ . By replacing another three extra tin atoms by mercury in a similar way, we get another orthorhombic structure of composition  $\text{HgSn}_{11}$ , and finally by replacing the remaining three tin atoms we get a rhombohedral structure of composition  $\text{HgSn}_8$ , the original rhombohedral symmetry of  $\text{HgSn}_{35}$  being restored (see Figure 4).

Later study has shown these conclusions to be not quite correct. To be sure, ordered structures of symmetry lower than rhombohedral can be obtained by replacing one or two of the "extra" tin atoms per layer per cell by mercury. If, however, the reasonable requirement is made that after such replacement all layers be crystallographically equivalent (a requirement no more unreasonable than the requirement that the same number of extra tin atoms be replaced by mercury in every layer) it can be shown that by replacing two extra tin atoms per layer per cell (to give  $\text{HgSn}_{11}$ ) either of two distinct ordered structures of rhombohedral symmetry are obtained, and no ordered structure of orthorhombic or lower symmetry. It can also be shown that by replacing one tin atom per layer per cell by mercury (to give  $\text{HgSn}_{17}$ ) either a monoclinic ordered structure or a rhombohedral

ordered structure can be obtained. The structures that would be obtained for  $\text{HgSn}_{11}$  and  $\text{HgSn}_{17}$  in these ways are shown in Figures 2 and 3. Of course, disordered structures, in which the "extra" tin atoms are replaced randomly by mercury, are possible, in which case it might be anticipated that the transition from  $\text{HgSn}_{35}$  to  $\text{HgSn}_8$  can be continuous and the symmetry rhombohedral over the entire range.

Professor Pauling suggested that powder photographs be taken to see if the diffraction lines for the hexagonal structure are split slightly as would in general be expected with conversion to true orthorhombic symmetry in the cases of  $\text{HgSn}_{17}$  and  $\text{HgSn}_{11}$ . In view of the large ratio of tin to mercury atoms it appeared far from certain that these distinctions could be made on the basis of superstructure lines on powder photographs, particularly in the alloys of lowest mercury content.

The object of the investigation reported here is to test Professor Pauling's hypothesis in the suggested way, although it is apparent from what has been said above that a splitting has a reasonable probability only in the case of  $\text{HgSn}_{17}$ , and will be found there only if the monoclinic superstructure exists for this composition.

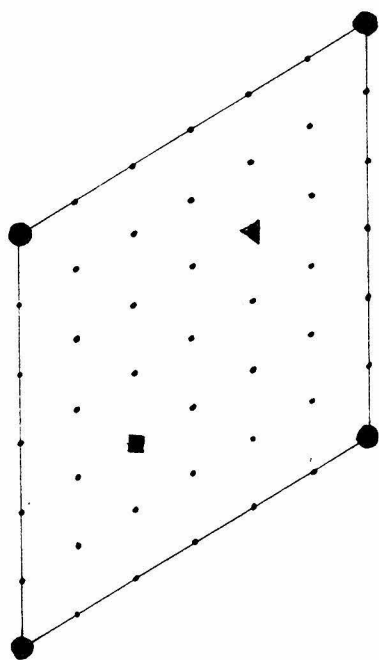
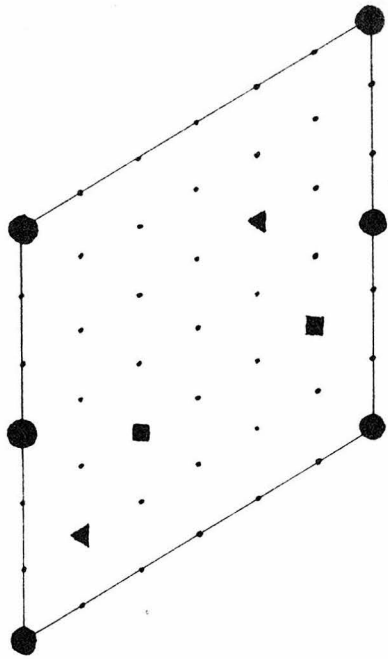
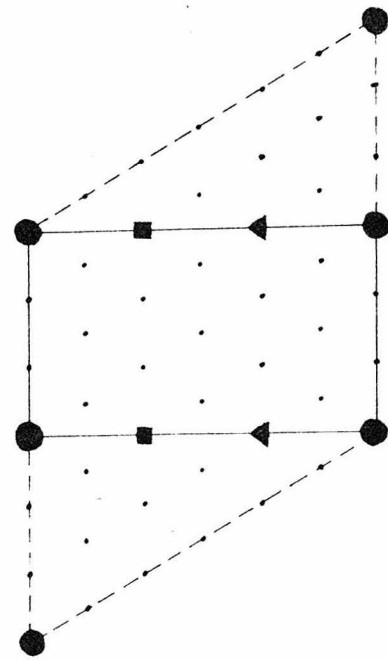


Figure 1. The hypothetical rhombohedral  $\text{HgSn}_{25}$  structure. Small dots represent tin atoms. Large dots, squares, and triangles represent mercury atoms in the planes  $z = 0$ ,  $z = 1/3$ , and  $2/3$  respectively.





(a)



(b)

Figure 2. (a) The hypothetical monoclinic  $\text{HgSn}_{17}$  structure. The original large hexagonal cell is shown with broken lines while the monoclinic cell is shown with full lines. Symbols as in Figure 1.  
(b) The hypothetical rhombohedral  $\text{HgSn}_{17}$  structure. Symbols as in Figure 1.

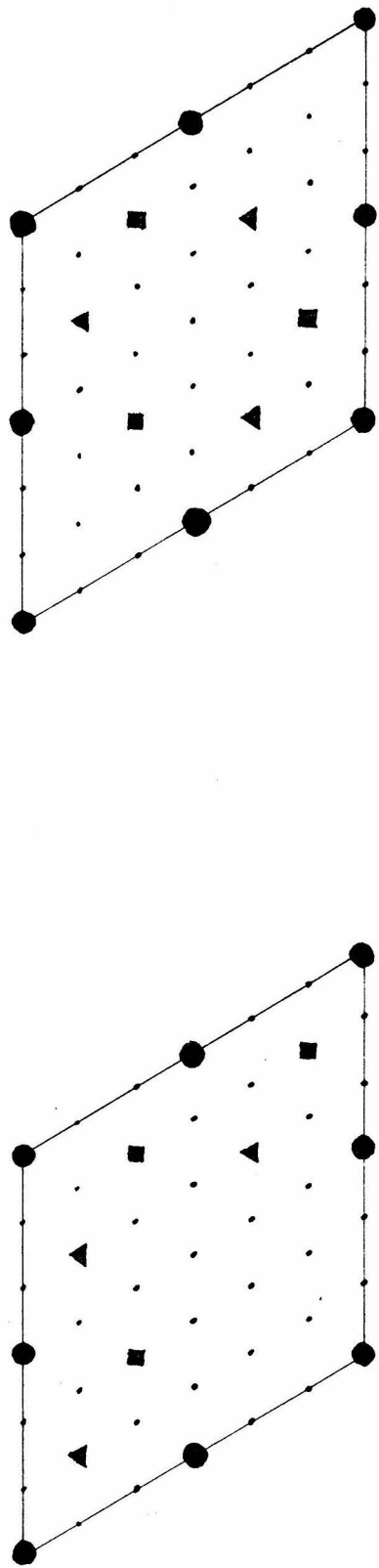


Figure 3. The two hypothetical rhombohedral  $\text{HgSn}_{11}$  structures. Symbols as in Figure 1.

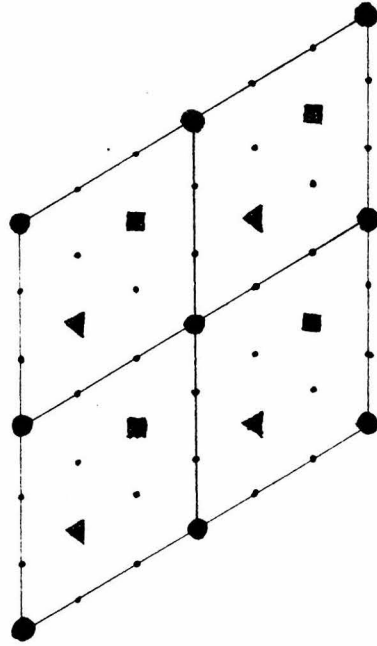


Figure 4. The hypothetical rhombohedral  $\text{HgSn}_8$  structure. The original large hexagonal cell has been transformed into four rhombohedral unit cells.

PREVIOUS WORK

According to Clara von Simson<sup>(1)</sup> tetragonal tin dissolves less than 2 at. % mercury (atomic percent) at room temperatures. If the amount of mercury is increased further a second phase shows up together with the tetragonal phase. This new phase has a structure based on a simple hexagonal lattice with one atom at each lattice point. It is the only solid phase when the total mercury content of the metal mixture exceeds approximately 6 at. %. Only these two structures were found. No indication was given as to the mercury content at which a liquid phase first appears. It was reported, however, that if the mercury content is 17% or more, the alloy can be separated into a solid and a liquid phase. The lattice constants of the solid phase are given as follows:

$$a_0 = 3.18 \text{ \AA.}, \quad c_0 = 2.99 \text{ \AA.}, \quad c/a = 0.94$$

F. Stenbeck<sup>(2)</sup> confirms von Simson's results, but adds that when the mercury content exceeds approximately 10 at. %, a third structure of orthorhombic symmetry appears. This orthorhombic structure is very closely related to the hexagonal one in that it can be considered as being formed from the latter by a very slight distortion. The lattice constants are given below:

At.% Hg	Lattice	a <sub>0</sub> Å.	b <sub>0</sub> Å.	c <sub>0</sub> Å.	a <sub>0</sub> :b <sub>0</sub> :c <sub>0</sub>
8	orthohex.	5.531	3.198	2.980	1.732: 1 :0.932
14	orthorhomb.	5.548	3.196	2.981	1.736: 1 :0.933

The most complete thermal investigation of this seems to have been made by Prytherch (unpublished). A phase diagram worked out by him is found in a report by M. L. V. Gayler<sup>(3)</sup>. This diagram is shown in Figure 5. In addition to the two phases reported by von Simson, Prytherch has also found a third phase which formed at about the same mercury content as that found by Stenbeck, but according to Prytherch this phase is stable only below approximately -35° C. An attempt to contact Mr. Prytherch for further information was not successful. Evidently the results reported by Stenbeck and Prytherch do not agree completely.

The work of Tammann and Mansuri<sup>(4)</sup> should also be mentioned. After a microscopic investigation <sup>these</sup> the authors found that in the range 0 to 18% mercury only one type of crystal is present. In a sample containing 20.6% mercury they could observe a liquid phase between the crystallites.

In view of this earlier work, it would appear at the outset that the hypothesis of Professor Pauling is probably incorrect, for no orthorhombic structures were reported to exist at the compositions required by that hypothesis. However, since nothing is known of the care or thoroughness with which these investigations were carried out, the work suggested by Professor Pauling was done as described below.

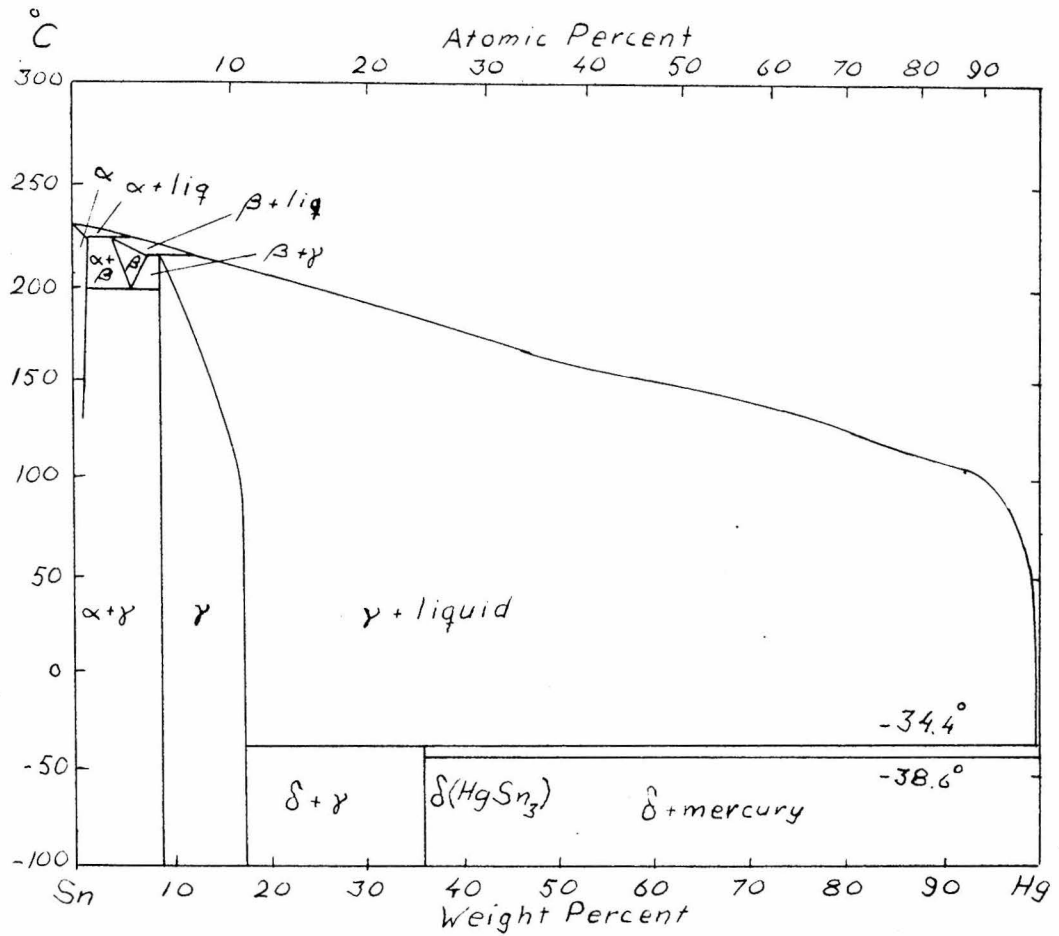


Figure 5. The Hg-Sn phase diagram (after W. E. Prytherch, unpublished, ref. 3).

## EXPERIMENTAL

Before the x-ray analysis was started, it was considered advisable to make a thermal analysis of mixtures having the compositions suggested by Professor Pauling, in order to obtain, if possible, confirmation of the existence of compounds having these compositions.

### Thermal Analysis

(a) Experimental equipment. The thermal analysis was performed in ampoules of the shape shown in Figure 6. Each ampoule was placed in a furnace so as to rest upon the bottom plug shown in Figure 7. The plug had a thermocouple junction immediately above the ampoule in order to make it possible to measure temperature differences in the furnace.

(b) Experimental procedure. Oxide-free tin metal was obtained by melting and casting the granulated tin used as starting material. The ampoules were charged with the proper amount of tin and mercury after having been filled with carbon dioxide, and were then sealed off. In order to obtain a homogeneous alloy, the samples were melted and shaken vigorously for about ten minutes and then allowed to solidify. All ampoules contained approximately the same amount of alloy.

Each analysis was made in the following way. One of the ampoules was placed in the furnace and the power turned on. The sample was heated to approximately 240° C. and kept at that temperature for about fifteen minutes. Part of the

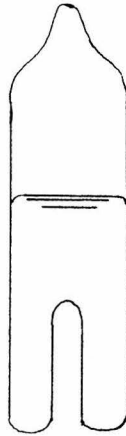


Figure 6. Glass ampoule used for thermal analysis.

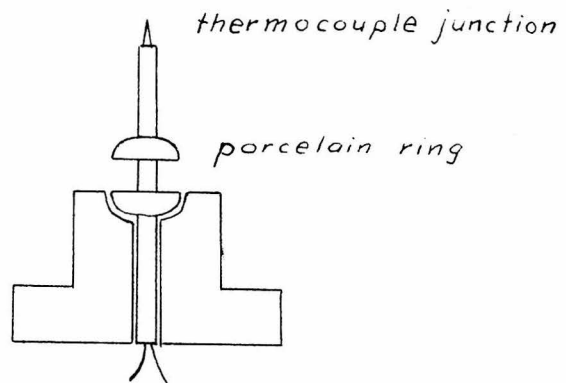


Figure 7. The bottom plug with thermocouple junction. The ampoule rests on the porcelain ring.



power was then turned off to obtain a slow cooling down (approximately 25° C. per hour). The temperature was carefully followed. Besides working with the four compositions previously mentioned, a thermal analysis was made also of pure tin in order to determine the operating characteristics of the equipment with a substance of known properties. The five temperature-time curves obtained in this way are given in Figure 8.

Results - The very pronounced supercooling made it difficult to obtain valuable information from the thermal analysis. However, the short or non-existent arrests and the comparatively gentle slopes following solidification make it appear that the alloy mixtures did not solidify to single, well defined compounds. As a matter of fact, a liquid phase could still be seen in the ampoules containing mixtures of overall compositions  $\text{HgSn}_8$  and  $\text{HgSn}_{17}$  when these ampoules were removed from the furnace at the completion of the runs (at the temperatures corresponding to the ends of the corresponding curves).

Much more information can probably be obtained from the thermal analysis by improving the technique, with special regard to eliminating the undercooling in some way.

#### X-ray Analysis

(a) Experimental equipment and experimental work. For the x-ray analysis, a powder camera of Straumanis type (Philips), 114.59 mm. in diameter, was used. The samples

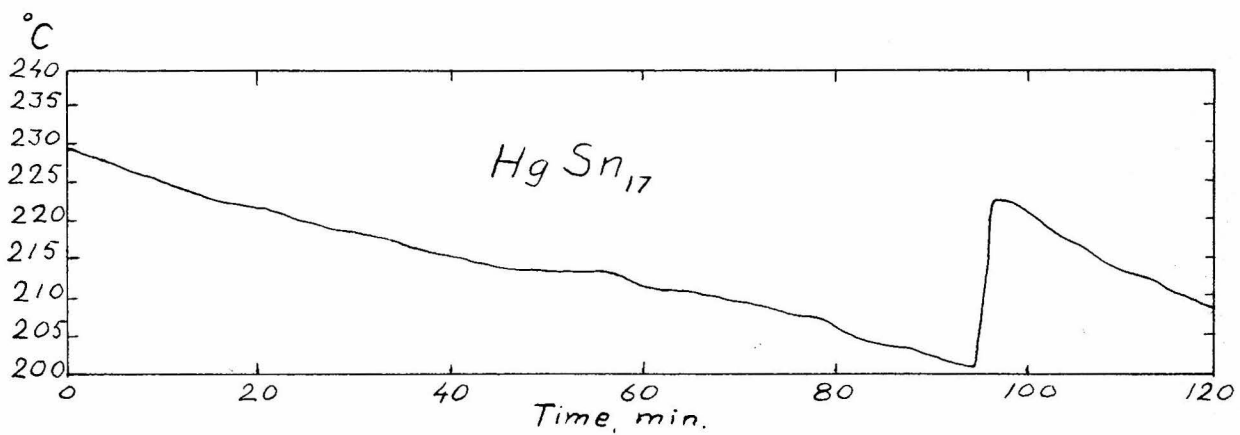
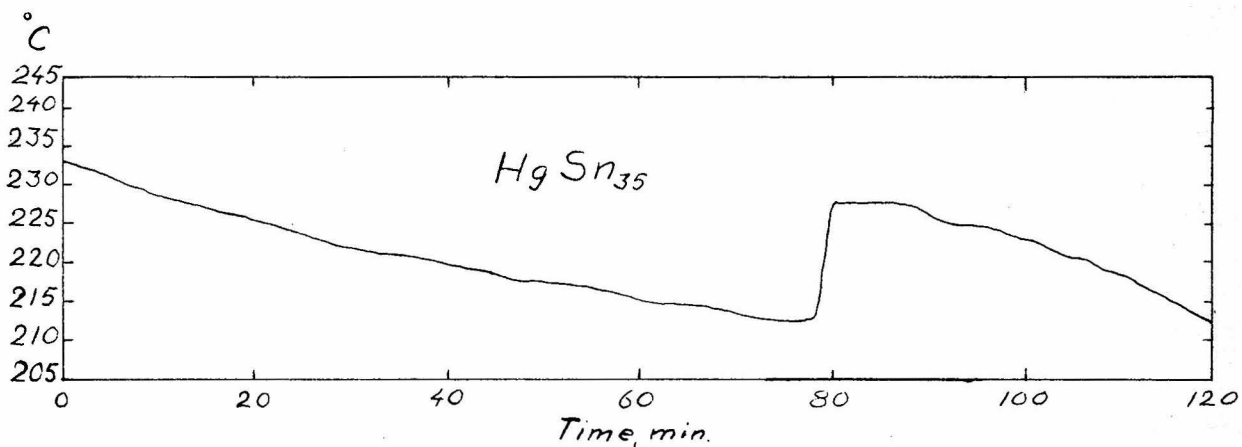
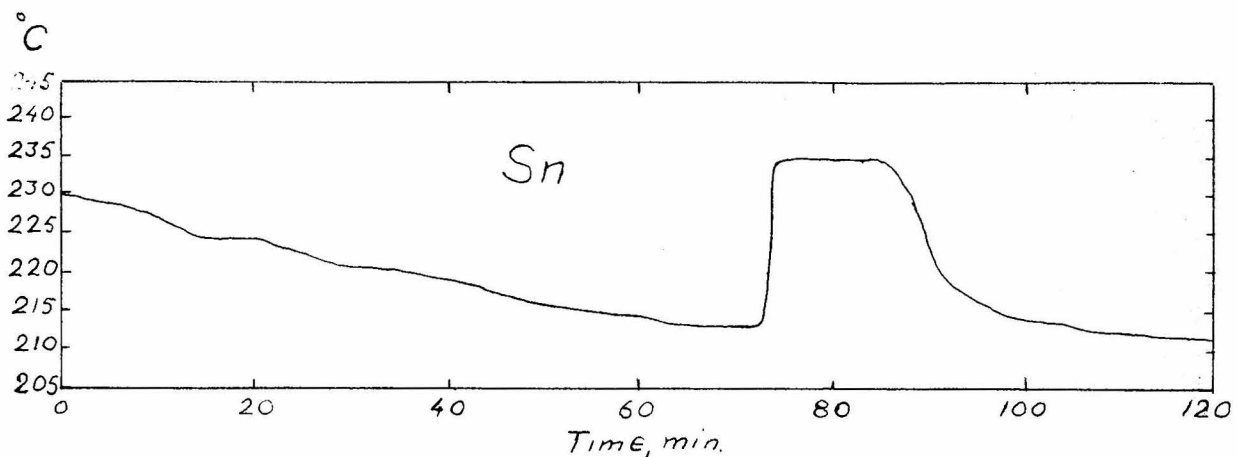


Figure 8. Cooling curves obtained for pure tin and the alloys of compositions HgSn<sub>35</sub> and HgSn<sub>17</sub>.

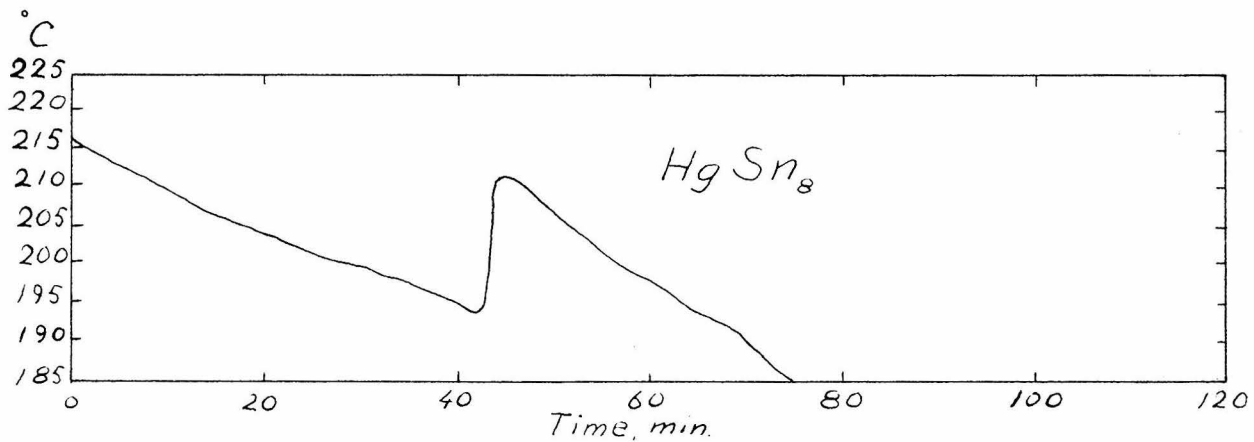
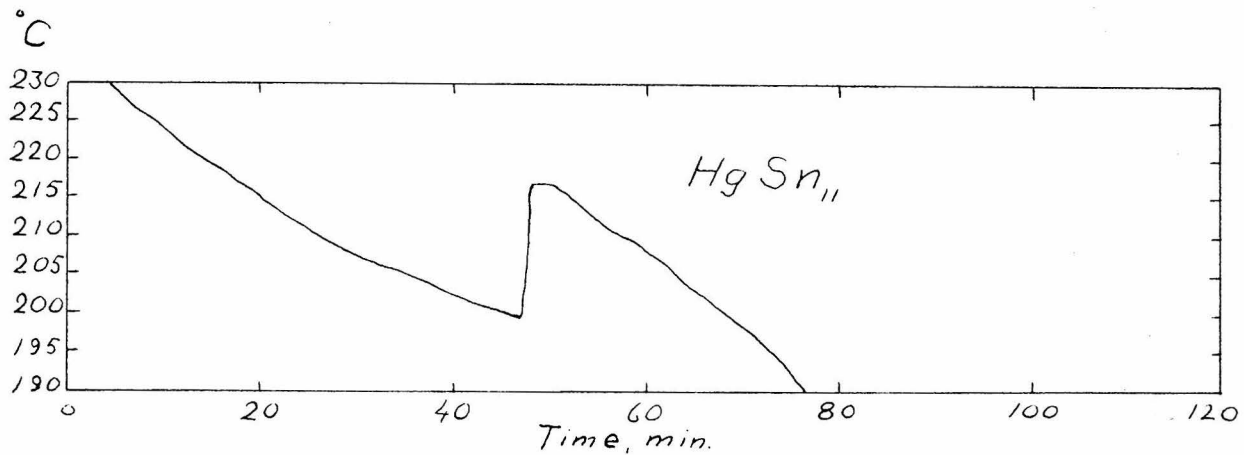


Figure 8 (continued). Cooling curves obtained for the alloys of compositions HgSn<sub>11</sub> and HgSn<sub>8</sub>.

were prepared by filing the metal slugs and passing the filings through a 325 mesh sieve. A very fine glass fibre, covered with a very thin layer of vaseline, was then coated with filings and the sample was ready to be photographed.

As to the preparation of the metal slugs, the experiences with the thermal analysis showed that a homogeneous slug is not obtained by letting the molten metal mixtures cool by themselves. For this reason, new samples were given a five weeks' annealing at 208° C. as a means of homogenizing them. The temperature was chosen as being well below the temperature of beginning solidification of all the mixtures. To reduce oxidation these new samples were sealed off in argon atmosphere.

Filings were taken from both the lower end and the middle part of the slugs. However, photographs of samples filed from both parts of a given slug often showed differences in the intensity relationships among the lines, indicating considerable inhomogeneity. Although in the case of a two or more phase system this is more or less to be expected, it was considered convenient to prepare a third series of samples by quenching the molten mixtures to "freeze in" a homogeneous structure. For comparison, one part could be annealed and photographs compared with those obtained of the simply quenched part.

The new samples (sealed off in vacuum to reduce oxidation still more) were quenched from 230° C. in cold water.

None of the pyrex ampoules cracked. The slugs were cut into two pieces. One half was put in a furnace and annealed for four weeks at 100° C., and the other used immediately for sample preparation, filings being taken from the cut end.

A new series of photographs was then taken, and also a photograph of pure tin. At this point it was also considered advisable to investigate a sample containing more than 10 at. % mercury, as Stenbeck reported a structure of orthorhombic symmetry for this composition in disagreement with Prytherch. A sample containing 15 at. % mercury was prepared and photographed as above.  $\text{CuK}\alpha$  radiation was used with a peak voltage of 36 kV on the tube. A nickel filter was used. The photographs obtained with the quenched and subsequently annealed samples are shown in Figure 9.

(b) Evaluation of the photographs. A close inspection of the photographs showed that the  $\text{HgSn}_8$  and  $\text{HgSn}_{11}$  samples had exactly the same set of lines and that the  $\text{HgSn}_{17}$  and  $\text{HgSn}_{35}$  samples had both this set of lines and a second set identical with the lines given by pure tin. The annealing of the samples had no effect on the diffraction patterns. From this was drawn the conclusion that only two phases are present in the composition range Sn -  $\text{HgSn}_8$ , in full agreement with earlier reports. The sample containing 15 at. % mercury gave a photograph of exactly the same type as that of  $\text{HgSn}_8$ . This is in agreement with Prytherch, but disagrees with Stenbeck.

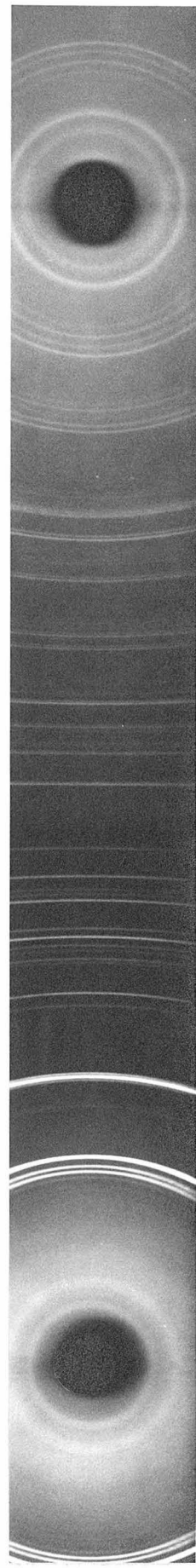
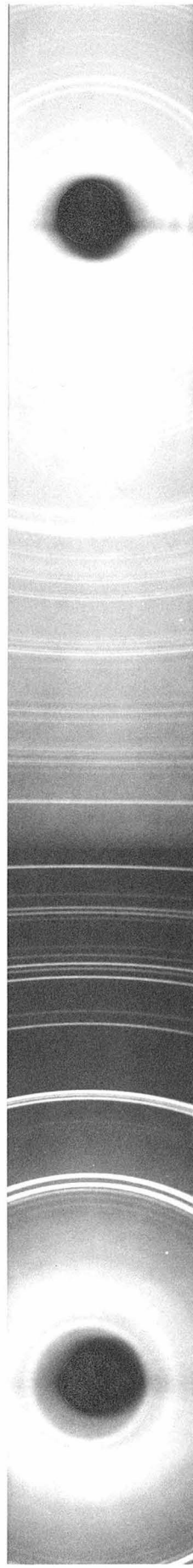
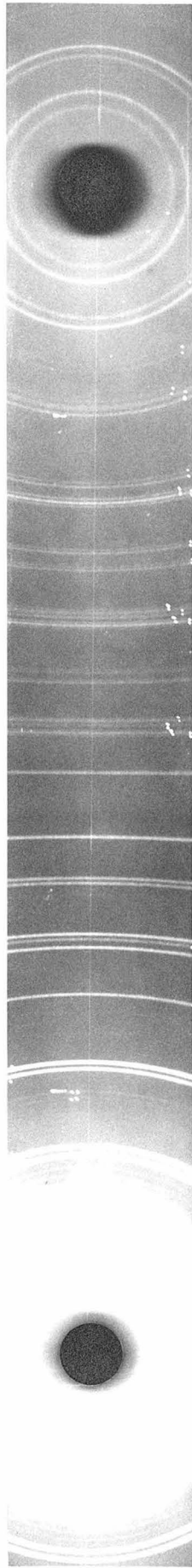
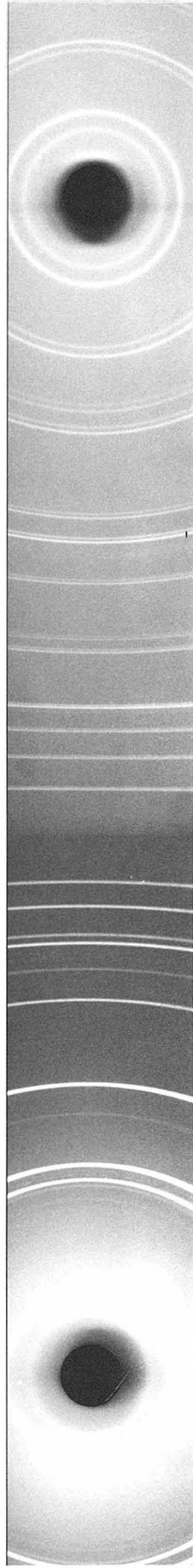


Figure 9. Powder photographs of pure tin and the alloys of compositions  $\text{HgSn}_{35}$  and  $\text{HgSn}_{17}$ .



-9b-

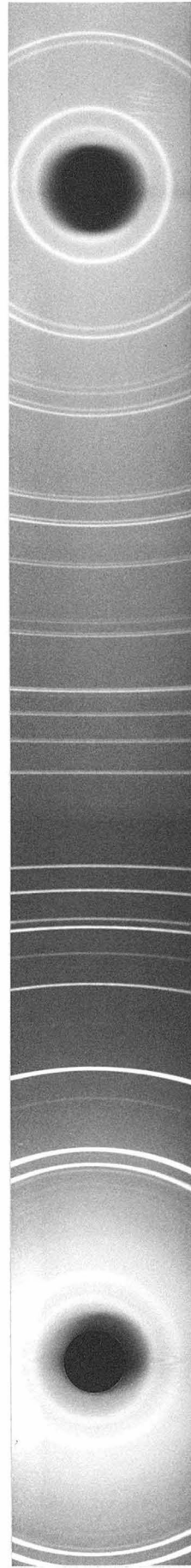


Figure 9 (continued). Powder photographs of the alloys of compositions  $\text{HgSn}_{11}$  and  $\text{HgSn}_8$ .

In order to find out what structure was present in the HgSn<sub>8</sub> sample and also to determine lattice constants of the two occurring structures in different mixtures, the photographs of tin and HgSn<sub>8</sub> were indexed and the positions of the lines measured. This was done on the assumption that the HgSn<sub>8</sub> structure was simple hexagonal with lattice constants given by Stenbeck, and tin tetragonal with lattice constants as given by Wyckoff.<sup>(5)</sup> With the exception of a few very faint lines and some fairly strong lines (the latter close to the central spot) all lines were explained by these two structures.

An attempt to explain the faint lines by assuming the presence of CuK $\beta$  radiation was completely successful in the case of tin and left only one very faint line unexplained on the HgSn<sub>8</sub> photograph.

Some fairly strong but very broad lines appeared to be explainable as bands due to white radiation limited on one side by the absorption edge of silver. In order to check this hypothesis, a photograph was taken of the HgSn<sub>8</sub> sample with a peak voltage of 23,000 volts. This voltage is too low to excite wave lengths corresponding to the silver absorption edge. This last photograph did not show any of these broad lines. Moreover the faint line which could not be indexed disappeared; this was quite possibly an impurity line (perhaps chromium), which disappeared as a result of replacing the x-ray tube. No line now remained which could



not be dismissed as being caused by something other than the simple hexagonal structure.

After this indexing it seems quite certain that only two different structures occur in the samples investigated, one identical with the tetragonal white tin structure, and one a simple hexagonal structure. No superstructure lines were observed, and none of the lines were split.

A matter of interest in this connection is the extent to which the lattice constants vary with varying amounts of mercury. For this reason, they were evaluated from all the photographs, including that of tin. A somewhat abbreviated least squares method was used. It would be interesting to know the lattice constants with greater accuracy. This could be done by improvement of the least squares method, but has not been done here because of the press of time. The results are found in Table I.

It may be seen from the table that the lattice constants of the tetragonal phase seem to have a slight tendency to decrease with increasing amounts of mercury.

TABLE I

Lattice Constants of Phases in Several Mercury-Tin Alloys

	Tetragonal		Hexagonal	
	$a_0$	$c_0$	$a_0$	$c_0$
Sn	5.818 Å.	3.173 Å.	---	---
HgSn <sub>35</sub>	5.813	3.171	2.984 Å.	3.205 Å.
HgSn <sub>17</sub>	5.812	3.168	2.980	3.209
HgSn <sub>11</sub>	---	---	2.983	3.207
HgSn <sub>8</sub>	---	---	2.982	3.203

-----  
Note: The dashes mean that the phase in question did not occur. The mean error is of the order 0.002 Å.

Discussion - The hypothetical compounds suggested by Professor Pauling do not seem to exist, with the possible exception of  $\text{HgSn}_8$ . Only a tetragonal structure (the same as in white tin) and a simple hexagonal structure have been observed, in full agreement with earlier reports. In alloys of calculated composition  $\text{HgSn}_{35}$  and  $\text{HgSn}_{17}$  both of these structures are present while in alloys of composition  $\text{HgSn}_{11}$  and  $\text{HgSn}_8$  and probably of any higher mercury content the hexagonal phase is the only solid phase present. The x-ray photograph of the  $\text{HgSn}_8$  mixture gave no superstructure lines that would indicate the suggested arrangement of the mercury atoms. However, any superstructure lines would be very weak, the intensity ratio between superstructure and substructure lines in this case being of the order of 250.

In the two structures mercury atoms seem to be able to take the places of tin atoms, possibly in a random way, with a slight decrease in the lattice constants. The solubility of mercury in the tetragonal phase is probably considerably less than one atom in thirty-six. No information as to the solubility of mercury in the hexagonal phase has been obtained as no third phase richer in mercury has appeared in this study. No clear evidence for the existence of a liquid phase was obtained in the x-ray analysis; the  $\text{HgSn}_8$  samples were, however, very soft and possibly contained some liquid phase.

The possibility still remains that the mercury atoms after a very long time will take some special positions in

the two structures. To find out whether this is so, it would probably be a good idea to make an x-ray analysis of filings that have been annealed for several weeks at 100° C. and make a very careful examination of the photographs for superstructure lines.

#### ACKNOWLEDGEMENT

I wish to express my gratitude to Professor Pauling for suggesting this study and for valuable discussions; to the Carbide and Carbon Chemicals Corporation for financial support of the program under which this work was done; and to Dr. David P. Shoemaker, under whose immediate direction this work was done, for advice and criticism.

#### SUMMARY

A brief study of the tin-rich side of the tin-mercury system has been made. Samples of the calculated compositions  $\text{HgSn}_{35}$ ,  $\text{HgSn}_{17}$ ,  $\text{HgSn}_{11}$  and  $\text{HgSn}_8$  have been studied by both thermal analysis and x-ray analysis. An additional sample containing 15 at. % mercury was studied by x-ray<sup>analysis</sup> only. Two different structures have been observed, one simple hexagonal and one tetragonal, the latter the same as in white tin. In the alloys of the compositions  $\text{HgSn}_{11}$  and  $\text{HgSn}_8$ , and also in the alloy containing 15 at. % mercury, the hexagonal structure was the only one present, while in the remaining two both structures were present. The solubility of mercury in

the tetragonal phase seems to be considerably less than 1 mercury atom for every 35 tin atoms. This study has not given any information as to the solubility of mercury in the hexagonal phase.

The four hypothetical compounds suggested by Professor Pauling do not seem to exist, with the possible exception of  $\text{HgSn}_8$ . Superstructure lines corresponding to the structure proposed for that compound have not been observed, however.

REFERENCES

1. C. von Simson, Z. phys. Chem., 109, 183 (1924).
2. F. Stenbeck, Z. anorg. allg. Chem., 214, 16 (1933).
3. M. L. V. Gayler, J. Inst. Metals, 60, 379 (1937).
4. G. Tammann and Q. A. Mansuri, Z. anorg. allg. Chem., 132, 66 (1923).
5. R. W. G. Wyckoff, "Crystal Structures", New York: Interscience Publishers, 1948. Paragraph (II,j).

PART II

THE DETERMINATION OF THE CRYSTAL STRUCTURE OF THE SIGMA  
PHASE BY THE APPLICATION OF X-RAY DIFFRACTION METHODS  
TO THIS PHASE IN THE IRON-CHROMIUM AND IRON-MOLYBDENUM  
SYSTEMS

INTRODUCTION

The so-called sigma phase occurs in systems of the transition group metals, particularly those of the first long period. It has been found to exist in a number of binary and ternary systems. It is a hard, brittle substance. Furthermore it is non-magnetic, at least in the iron-chromium system<sup>(1,2)</sup>, notwithstanding the presence of ferromagnetic elements in all of these phases. In binary systems it usually occurs in the neighbourhood of a 1:1 atomic ratio but ordinarily has a composition range of the order of 5 - 10 atomic percent. In binary systems in which it is known to occur it is usually stable at room temperature. However, it cannot always be formed directly from the melt, as the phase stable at the melting point is often the alpha phase (body-centered cubic). As an example the phase diagram of the Fe $\bar{\chi}$ Cr system is shown in Figure 1<sup>(1)</sup>. The phase forms with extreme slowness at room temperature but can be formed from the alpha phase at temperatures just below the alpha-sigma transition temperature in a few days or weeks. The phase is most easily identified<sup>(3)</sup> by its x-ray powder diagram, which is very characteristic.



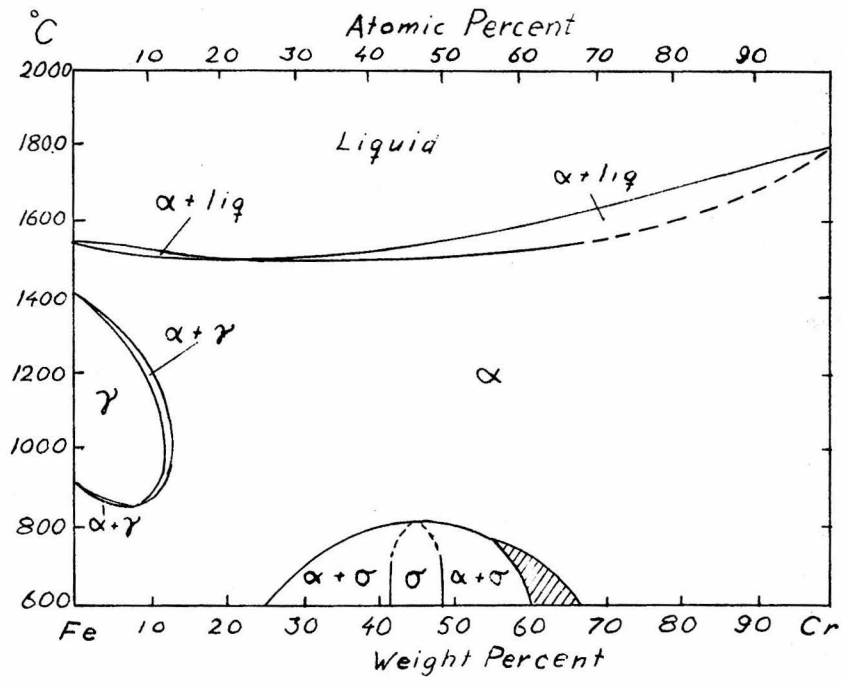
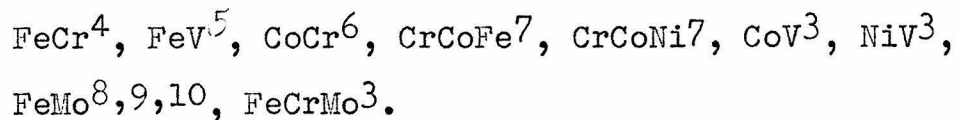


Figure 1. The Fe-Cr phase diagram (Metals Handbook, ref. 1).

The sigma phase is of great technological importance. It is known to occur in stainless steels where it has been found to reduce impact strength and resistance to corrosion. It is also of considerable theoretical importance because of its brittleness and the absence of ferromagnetic properties, and because of the apparent complexity of its structure (as indicated by the complexity of the powder diagrams). In the FeCr and FeV systems, at least, it appears to be the only phase having a complex structure.

Because of the great technological and theoretical importance of the sigma phase, the structure has long been sought for by many workers, all without success up to the time of the structure determination to be here described. In particular Professor Linus Pauling has for several years been interested in the sigma phase and desirous of having its structure determined. It is largely because of his interest that the work described here was done.

Previous work on the sigma phase has consisted mainly of determining in what alloy systems the phase occurs. The occurrence of the sigma phase has been established in the following metal systems:



Duwez and Baen<sup>(3)</sup> have formulated the following empirical rules for the occurrence of the sigma phase in binary systems:

1. The atomic radii of the two elements must not differ by more than eight percent. (The radii should be taken for coordination number twelve.)

2. One of the two metal constituents must have in its elementary state a body-centered cubic structure and the other a face-centered cubic structure at least in one of their respective allotropic forms.

These two rules hold for all the binary systems mentioned above except the FeMo-system; in this case the radius of molybdenum is slightly too large compared to that of iron to fall within the eight percent limit. Hence, if the first rule were modified only slightly, the FeMo-system would no longer be an exception. As a very great number of binary systems have not yet been investigated in order to find a sigma phase it is still too early to establish the value of these rules.

Although there have probably been many attempts to determine the crystal structure of the sigma phase only a few are described in the literature. They are all based on powder work. According to Bradley and Goldschmidt<sup>(1)</sup> the sigma phase in the FeCr-system appears to have a complex body-centered cubic structure. According to the same authors, two modifications appear to occur, one stable and one transitional. In an x-ray study by Duwez and Baen<sup>(3)</sup> of this Institute, primarily undertaken to obtain standard powder patterns of the sigma phase in different metal systems, an attempt

was also made to find the unit cell for the sigma phase on the basis of calculated interplanar spacings. When a specially designed Hull-Davey chart for the tetragonal system was tried a promising but not particularly good fit was found for an axial ratio  $c:a$  near 1.46 (approximately the same value for all the investigated systems). For sigma FeCr the axial lengths found were:  $a = 6.196 \text{ \AA}$  and  $c = 9.058 \text{ \AA}$ . The calculated number of atoms in the unit cell of the iron-chromium sigma phase was approximately thirty (29.7). Pietrokowsky<sup>(12)</sup> in continuing the work on the sigma phase begun by Duwez and Baen, seemed to be successful in indexing the sigma powder pattern in the FeCr-system on the basis of an orthorhombic unit cell. The lattice constants he obtained were:

$$a = 8.66 \text{ kX.}, \quad b = 6.21 \text{ kX.}, \quad c = 5.18 \text{ kX.}$$

With these lattice constants the number of atoms in the unit cell was calculated to be approximately twenty four (23.82). The agreement between calculated and observed interplanar distances for this cell was better than that for the tetragonal cell but still left something to be desired. Due to the very high degree of similarity between different sigma patterns it was also possible to index powder patterns from other metal systems with the same qualified success. No attempt to carry out a complete structure determination has been reported by this group of workers.

It was as a result of a visit by Mr. Paul Pietrokowsky of this Institute (Jet Propulsion Laboratory) in the spring of 1950 that we became actively interested in determining the structure of the sigma phase. When Professor Duwez and Mr. Pietrokowsky became aware of our interest in this problem they kindly made available to us several powder photographs of several sigma phase compounds, as well as powder samples of sigma-FeCr.

Before any direct work was done in this Laboratory to collect additional data and determine the structure, Professor Pauling made two attempts to propose a structure that would fit previously reported lattice constants. These attempts gave structures which, on closer examination and consideration of the available data, proved to be incorrect.

The first structure proposed by Professor Pauling was designed to fit the orthorhombic unit of Pietrokowsky. It contained two groups of twelve atoms each, one centered at (000) and the other at  $(\frac{1}{2}\frac{1}{2}\frac{1}{2})$ . Each group was obtained from the twenty six atom group found in the gamma alloys (e.g. gamma brass,  $\text{Cu}_5\text{Zn}_8$ ) by removing peripheral atoms until the only ones left were the positive and negative tetrahedra and four of the six atoms in the octahedron; this group was rotated around the a-axis so that the axis from which the octahedral atoms were omitted made an angle of approximately  $35^\circ$  with the z-direction. The group at  $(\frac{1}{2}\frac{1}{2}\frac{1}{2})$  was related to that at (000) by n-glides to give space

group P 2nn. However, strong reflections occurred<sup>r</sup> which, when indexed with reference to this cell, ruled out the space group, and furthermore a model of this structure failed to show satisfactory packing among the groups.

Another structure was proposed later by Professor Pauling which had a 28-atom body-centered tetragonal unit with axial lengths slightly less than those of the thirty-atom unit reported by Duwez and Baen. This structure made use of two fourteen atom units, each containing an inner positive tetrahedron of atoms, a negative tetrahedron of atoms outside of that, and finally an octahedron of atoms outside the negative tetrahedron, to give a group identical to that in gamma brass except that the twelve peripheral atoms of the latter were missing. These groups were supposed to be centered at (000) and  $(\frac{1}{2}\frac{1}{2}\frac{1}{2})$  with one of the octahedral axes of each group parallel to the c-axis and with the others at  $26.5^\circ$  to the a- and b-axes. Dr. Shoemaker showed that this structure contains holes at  $(0\frac{1}{2}\frac{1}{4})$  and  $(\frac{1}{2}0\frac{3}{4})$  which require the presence of two more atoms per unit cell giving a total of thirty. The resulting structure indeed appeared to be a very reasonable one but was not applicable to the sigma phase. The sigma powder pattern when indexed on the basis of the tetragonal cell of Duwez and Baen did not show the absences required by a body-centered structure. Moreover strong planes that were predicted for the proposed structure were weak or unobserved.

At this point it was decided that an attempt be made to obtain powder data of greater precision on the basis of which an improved indexing of the lines might be achieved. In retrospect it appears very likely that this could have been done, for the unit cell that was later found was very closely related to that found by Duwez and Baen, having a c-axis about half as long and an a-axis about  $\sqrt{2}$  times as long as the corresponding axes of the cell of Duwez and Baen. Moreover, it appears likely that had the unit cell been found from the powder photographs, the crystal structure might have been found through the same considerations that were employed in the single crystal work. However, two fortunate circumstances led quickly to the use of single crystal techniques. The powder sample of sigma-FeCr that was used for obtaining powder patterns was not finely ground, and the rotation drive on the camera failed, with the result that very grainy powder lines were observed on the photograph (see Figure 2). The grainy character of the lines suggested the possibility of isolating single crystals from the powder sample and applying single crystal techniques. In fact this was found possible and the structure of the sigma phase was quickly found through single crystal work in the way described in the pages to follow.



Figure 2. Powder photograph of coarsely ground  $\sigma$ -FeCr.



## EXPERIMENTAL

Materials. Professor Duwez kindly furnished us with a powder sample of FeCr-sigma that had been prepared in the following way. 325-mesh chromium powder and likewise 325-mesh iron powder were carefully mixed in the atomic proportions 1:1 and then compressed to a pellet. The pellet was then sintered in vacuum at 1200° F. for ten days and allowed to cool down. The pellet was crushed to a powder which was annealed at 1200° F. for one hour. An analysis of the powder prepared in this way gave 46.5 atomic percent chromium. The density of an iron-chromium sigma phase of very nearly the same composition had been determined earlier by Duwez and Baen. They found the value  $7.600 \pm 0.005$ .

### Preliminary powder work

(a) Equipment. For the powder work described in this thesis a Straumanis powder camera (Philips) of diameter 114.59 mm. was used. Eastman "No Screen" x-ray film was used throughout. The radiation used was  $\text{CuK}\alpha$ , with nickel filter.

(b) Preparation of powder samples. A glass fibre about 0.02 mm. in diameter was mounted with shellac on the brass pin of standard type<sup>used</sup> in this Laboratory for powder work. The glass fibre was then coated with a thin layer of vaseline. Thus prepared it was dipped repeatedly but lightly in the sigma powder described above. In this way the glass fibre was covered with a thin, smooth layer of powder particles.

(c) Exposures. The first photograph was exposed for about twelve hours. Although a few strong lines could be observed the background was so strong as to make the photograph practically without value for measurements. The background was presumably caused by fluorescence from the sample. This fluorescent radiation was successfully eliminated by placing a nickel filter in contact with and inside the film in the camera. Due to the usage of two filters an exposure of 100 hours was necessary for a good photograph. The exposure could no doubt have been made considerably shorter with the same good result if the primary nickel filter had been removed. A typical photograph is shown in Figure 2. The graininess of the lines is so prominent as to make the photograph rather unfit for exact measurements but it also rather strongly suggests attempts to find single crystals. As was mentioned in the introduction the powder work was interrupted at this point for this very reason and a search for single crystals was initiated.

The search for single crystals - A small quantity of the powder sample given to us by Professor Duwez was spread out in a very thin layer on a glass slide. When examined in a microscope with a linear magnification of 36 a great number of individual particles were observed, the average size of which was of the order 0.01 mm. Under the microscope a few particles of a shape that seemed to indicate single crystals were isolated by moving away all neighboring

particles. The selected particles were then mounted on glass fibers affixed to brass pins of the type used in the powder work. The procedure was as follows. The end of the glass fibre was dipped in a solution of shellac in alcohol so that a droplet of the solution was formed at the end of the fibre. When one of the selected particles was touched with the droplet it generally adhered to it. The shellac was then allowed to dry for an hour or so.

Laue photographs were then taken. White radiation was used with a camera distance of 5 cm. In general a one hour exposure was sufficient. On most of the photographs obtained in this way a great number of spots were observed very often in clusters with the spots so close to each other that there was good reason to believe that a large number of single crystals were present. Crystals giving such photographs were immediately discarded. A few particles - the fourth and the sixth one - gave Laue photographs that contained a very limited number of spots all well apart from each other. After being reoriented a number of times these particles gave Laue photographs that possessed mirror planes. It was therefore certain that they were single crystals or perhaps twinned single crystals. In the following pages these particles will be called Crystal No. 4 and Crystal No. 6 respectively.

Description of the single crystals - Crystal No. 4 had the shape of a needle about 0.05 mm. long and about 0.02 mm. thick. The needle axis bore no apparent relation to the

crystal axes. It completely lacked well developed faces.

Crystal No. 6 had the shape of a rather thick rhombic flake with the rhombic edges about 0.04 mm. long and a thickness of about 0.02 mm. This crystal also lacked well developed faces.

The Laue symmetry of the sigma phase crystal structure - After the appearance of a mirror plane on a Laue photograph obtained with Crystal No. 4 additional symmetry elements were sought for. This was done by rotating the crystal a small angle around an axis normal to the mirror plane, taking a Laue photograph, and repeating the process until a second mirror plane was found normal to and non-equivalent to the first one (see Figure 3). When the crystal was rotated  $90^\circ$  from this position around the same axis a Laue photograph was obtained that was identical with the preceding one. This established the Laue symmetry as  $D_{4h}$ .

The results obtained with Crystal No. 4 were fully confirmed by the results obtained from Crystal No. 6. By proceeding as described above for Crystal No. 4, a Laue photograph was obtained that was identical with the photograph shown in Figure 3. Fortunately this crystal happened to be oriented on the glass fibre in such a way that it could easily be exposed with the four-fold axis parallel to the x-ray beam. The result of this exposure is shown in Figure 4. The presence of a four-fold axis was thus confirmed and also the Laue symmetry  $D_{4h}$  arrived at above.

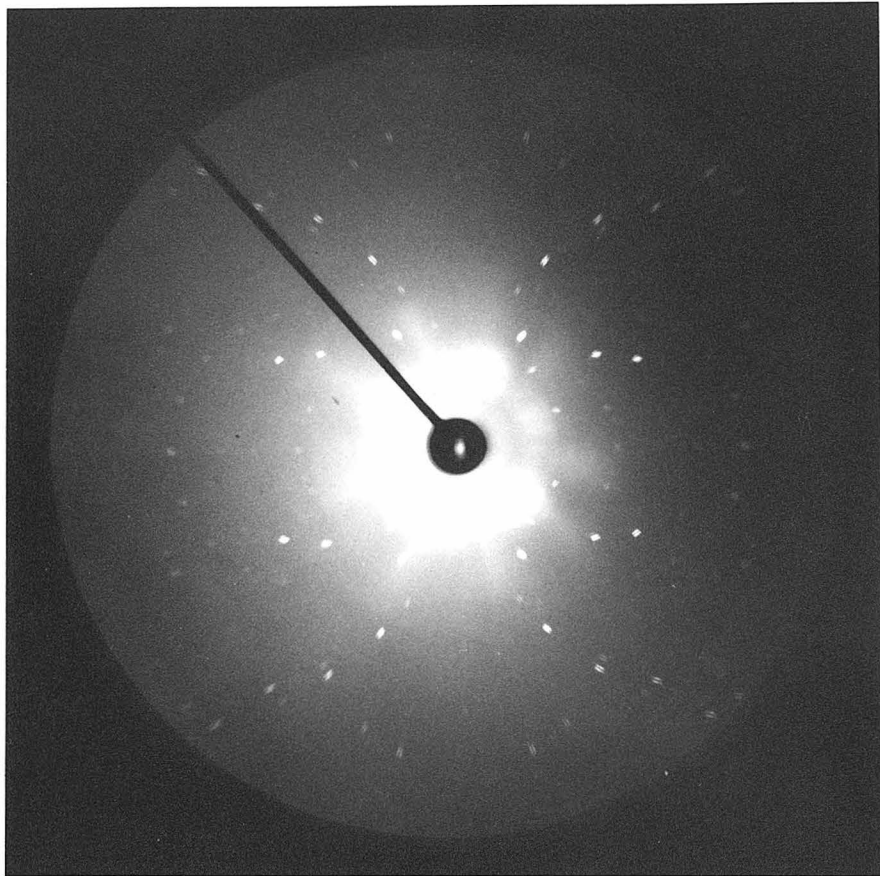


Figure 3. Laue photograph of  $\sigma$ -FeCr. X-ray beam parallel to the bisectrix of  $a$  and  $b$ ;  $c$  horizontal.

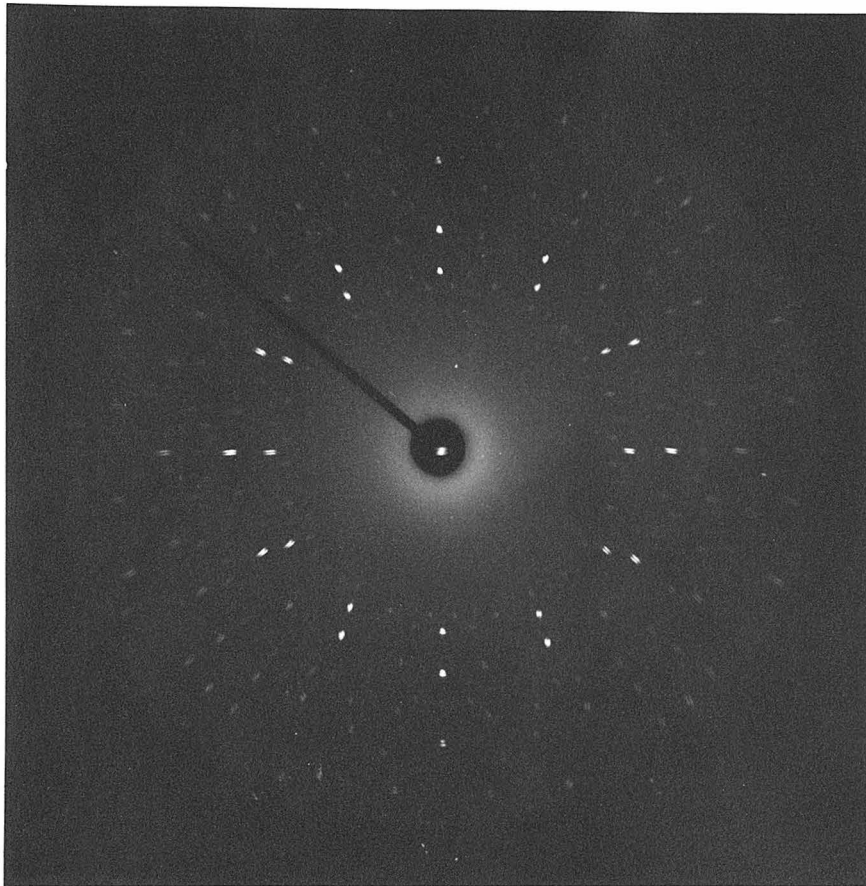


Figure 4. Laue photograph of  $\sigma$ -FeCr. X-ray beam parallel to  $\tilde{c}$ ;  $\tilde{a}$  at an angle of  $45^\circ$  with the horizontal.

A very striking feature of the photograph shown in Figure 4 is the pseudo-twelve-fold symmetry axis. This peculiarity immediately attracted our attention and made us strongly suspect that the crystal structure of the sigma phase is some way or other built up from two pseudo-hexagonal substructures turned  $90^\circ$  with respect to each other. That this was later found essentially correct will be shown in subsequent pages.

It followed immediately from the established Laue symmetry that the symmetry of the crystal lattice (the crystal symmetry) is tetragonal provided that twinning does not occur. A discussion of this possibility will be given in a later section.

The approximate determination of unit cell dimensions - When the symmetry of the crystal lattice had been determined, the next problem was to find the unit cell dimensions. This could quite easily have been done on the basis of the information provided by the Laue and powder photographs. It was decided, however, that the easier and more straightforward method of using rotation photographs should be used.

(a) Equipment. The rotation photographs were obtained with a 30.2 mm. <sup>(radius)</sup> rotation oscillation camera.  $\text{CuK}\alpha$  radiation (Ni-filter) was used.

(b) Procedure. For the Laue exposures Crystal No. 4 had already been oriented with its c-axis vertical. It could consequently be used without reorientation for a c-rotation

photograph. Crystal No. 6 had been oriented with its c-axis horizontal and a symmetry plane horizontal. It could therefore also be used for a rotation photograph without reorientation.

(c) Calculations. The easily deduced formula for determination of repeat distances from layer line measurements is as follows:

$$r = \frac{n \lambda}{\sin(\text{tg}^{-1} d/2R)}$$

where r is the repeat distance, R the camera radius,  $\lambda$  the wave length of the radiation, d the distance between two corresponding layer lines and n the order of the layer lines.

By application of this formula the following results were obtained.

$$a'_0 = 12.46 \text{ \AA}.$$

$$c_0 = 4.58 \text{ \AA}.$$

The prime is used because it was not known whether the a-axis was vertical in Crystal No. 6 or whether it made an angle of  $45^\circ$  with the vertical.

In order to settle the question as to whether the true a-axis is of length 12.46 A. or that value divided by the square root of two, a Weissenberg photograph (hk0) was taken around the four-fold axis of Crystal No. 4. The resulting photograph contained very few spots and could not be indexed



by inspection; consequently it was necessary to measure the positions of the spots and plot out the reciprocal lattice layer by calculation. The largest square reciprocal lattice net to which the observed planes could be fitted corresponded to  $a_0 = 8.82 \overset{\circ}{\text{Å}}$ . Unless there are (hk0) extinctions due to body-centering or to an n-glide plane, this is the true value of the lattice parameter. The primitive character of the lattice and the absence of an n-glide plane normal to c were established by indexing both the  $l = 0$  and  $l = 1$  layer line on the rotation photograph taken with Crystal No. 4; it was found that the same net that was found suitable for the indexing of  $l = 0$  also sufficed for  $l = 1$ . Moreover, since Bragg angles observed on the zero layer of the rotation photograph were found to be in good agreement with Bragg angles for certain observed lines on the powder photograph, there was little doubt that the single crystals selected for this work were crystals of the sigma phase. All remaining doubt was later removed when it was found possible to index the powder photograph completely on the basis of lattice parameters close to those obtained in the single crystal work, and when it was found that the intensity relationships among the powder lines were compatible with the intensities obtained in the single crystal work.

The refinement of the unit cell dimensions - It was decided that the refinement of the cell dimensions be made on the basis of powder data with the application of a least squares method.

(a) Preparation of powder photographs. As was mentioned in an earlier section very grainy powder photographs were obtained with the powder sample. They were in fact so grainy that they did not seem very suitable for exact measurements. For this reason some more photographs were taken using a more finely ground powder. Indeed, the powder lines became quite smooth but no powder lines could be observed at large Bragg angles where they were needed for accurate determination of the cell dimensions. With the coarser powder used at first we had obtained photographs with easily observable lines at all angles, however. In spite of their graininess we therefore decided to make the necessary measurements on one of those photographs.

(b) Indexing of the powder photograph. For a tetragonal crystal the following equation holds

$$Q = \frac{1}{d^2} = \frac{1}{a^2} (h^2 + k^2) + \frac{1}{c^2} l^2 \quad \text{eq. 1}$$

where  $d$  is the interplanar distance. The quantity  $Q$  thus appears to be the most convenient quantity to work with for the indexing as well as for the least squares treatment. The positions of the powder lines were measured with

a precision steel rule and from these measurements the Q-values were calculated. The results are presented in Table I under  $Q_{\text{obs}}$ . When Q values were calculated according to equation 1. on the basis of the cell dimensions obtained from rotation photographs and presented earlier, it was possible to index a great number of lines unambiguously. Many lines could not be indexed, however, but by adjusting cell dimensions in a way suggested by the differences between observed and calculated Q-values for the lines that had already been indexed, it was possible to index many of them. By repeating this procedure a few times it was possible to index all lines. The cell dimensions that were obtained by this method of successive adjustments were

$$a_0 = 8.798 \text{ \AA} \quad c_0 = 4.546 \text{ \AA}.$$

(c) Least squares refinement. For the least squares refinement equation 1. is conveniently written

$$Ax + By = Q \quad \text{eq. 2}$$

where

$$A = h^2 + k^2 \quad B = l^2 \quad x = \frac{1}{a^2} \quad \text{and} \quad y = \frac{1}{c^2}$$

With the observational equations of the linear form of equation 2. the two normal equations are

$$\begin{aligned} [wAA] x + [wAB] y &= [wAQ] \\ [wAB] x + [wBB] y &= [wBQ] \end{aligned}$$

where the brackets stand for summation over all planes and  $w$  is the weight of the observation for a given plane.

The weight of an observation was determined in the following way. We have

$$Q = \frac{1}{d^2} \propto \sin^2 \nu^{\theta}$$

If we differentiate, we obtain

$$dQ \propto \sin 2\nu^{\theta} d\nu^{\theta} \quad \text{eq. 3}$$

Now it is reasonable to assume that the position of a powder line can be measured with approximately the same accuracy at whatever Bragg angle it is measured, with the possible exception for Bragg angles close to  $90^\circ$  where lines may be broad and difficult to measure. This also means that the accuracy with which the Bragg angle can be determined is independent of where the corresponding line is situated on the film. From equation 3. we can then conclude that the standard deviation  $\sigma_Q$  in the determination of  $Q$  will satisfy the relation

$$\sigma_Q \propto \sin 2\nu^{\theta}$$

But we also have

$$w_Q \propto \frac{1}{\sigma_Q^2}$$

where  $w_Q$  is the weight of the observation.

TABLE I

Agreement between Observed and Final Calculated

Q-Values for Powder Lines

Indices	$w_Q$	$Q_{obs}$	$Q_{calc}$	$(Q_{obs} - Q_{calc}) \times 10^4$
002	1.6	0.1948	0.1937	11
330	1.5	.2340	.2325	15
202	1.4	.2453	.2454	- 1
212	1.4	.2581	.2583	- 2
411	1.4	.2678	.2680	- 2
331	1.3	.2827	.2809	18
222	1.3	.2974	.2970	4
312	1.3	.3234	.3229	5
322	1.2	.3610	.3616	- 6
431	1.2	.3728	.3713	15
511	1.2	.3851	.3842	9
432	1.1	.5174	.5166	8
522	1.1	.5675	.5682	- 7
532	1.0	.6319	.6328	- 9
550	1.0	.6462	.6457	5
413	1.0	.6547	.6554	- 7
333	1.0	.6677	.6683	- 6
720	1.0	.6835	.6845	-10
622	1.0	.7106	.7103	3
721	1.0	.7321	.7329	- 8
513	1.0	.7716	.7716	0
414	1.0	.9924	.9944	-20
751 $\alpha_1$	1.0	1.0027	1.0041	-14

TABLE I (continued)

Indices	$w_Q$	$Q_{obs}$	$Q_{calc}$	$(Q_{obs} - Q_{calc}) \times 10^4$
751 $\alpha_2$	1.0	1.0038	1.0041	- 3
802 $\alpha_1$	1.0	1.0182	1.0203	-21
802 $\alpha_2$	1.0	1.0196	1.0203	- 7
742 $\alpha_1$	1.0	1.0337	1.0332	5
742 $\alpha_2$	1.0	1.0343	1.0332	11
921 $\alpha_1$ 761 $\alpha_1$	1.1	1.1452	1.1462	-10
921 $\alpha_2$ 761 $\alpha_2$	1.1	1.1460	1.1462	- 2
405 $\alpha_1$	1.2	1.4168	1.4173	- 5
415 $\alpha_1$	1.3	1.4244	1.4302	-58
415 $\alpha_2$	1.3	1.4236	1.4302	-66
10.3.1 $\alpha_1$	1.4	1.4555	1.4561	- 6
10.3.1 $\alpha_2$	1.5	1.4560	1.4561	- 1
10.0.2 $\alpha_1$ 862 $\alpha_1$	1.6	1.4847	1.4852	- 5
10.0.2 $\alpha_2$ 862 $\alpha_2$	1.6	1.4846	1.4852	- 6
960 $\alpha_1$	1.7	1.5122	1.5110	12
960 $\alpha_2$	1.7	1.5120	1.5110	10
961 $\alpha_1$	1.9	1.5602	1.5595	7
961 $\alpha_2$	1.9	1.5587	1.5595	- 8
11.1.0 $\alpha_1$	2.0*	1.5760	1.5756	4
11.1.0 $\alpha_2$	2.0*	1.5761	1.5756	5
10.5.0 $\alpha_1$ 11.2.0 $\alpha_1$	2.0*	1.6147	1.6143	4
10.5.0 $\alpha_2$ 11.2.0 $\alpha_2$	2.0*	1.6158	1.6143	15

TABLE I (continued)

Indices	$w_Q$	$Q_{obs}$	$Q_{calc}$	$(Q_{obs} - Q_{calc}) \times 10^4$
11.1.1 $\alpha_1$	2.2*	1.6238	1.6240	- 2
11.1.1 $\alpha_2$	2.2*	1.6237	1.6240	- 3
535 $\alpha_1$	2.8*	1.6489	1.6498	- 9
535 $\alpha_2$	2.8*	1.6489	1.6498	- 9
11.2.1 $\alpha_1$ 10.5.1 $\alpha_1$	3.5*	1.6633	1.6628	5
11.2.1 $\alpha_2$ 10.5.1 $\alpha_2$	3.5*	1.6630	1.6628	2

-----  
\* Adjusted figure; takes account of broadness of lines  
at large angles.

We finally obtain

$$w_Q \propto \frac{1}{\sin^2 2\theta} \quad \text{eq. 4}$$

A few observations with Bragg angles close to  $90^\circ$  were given smaller weights than calculated with equation 4. as the corresponding lines were considerably broad and hard to measure accurately.

When the least squares refinement was carried out as outlined above the following results were obtained:

$$a_0 = 8.7995 \pm 0.0004 \text{ \AA.} \quad c_0 = 4.5442 \pm 0.0020 \text{ \AA.}$$

( $\lambda_{CuK\alpha, \alpha_2} = 1.5418 \text{ \AA.}$ )

The uncertainties given are probable errors.

Values of Q calculated on the basis of these cell dimensions are found in Table I.

The results above were obtained with <sup>the</sup> assumption that absorption errors are negligible. This assumption seems a priori reasonable on the basis of experience obtained in this Laboratory with powder samples of comparable dimensions and scattering power. Examination of the final residuals  $\Delta Q$  at large scattering angles, where absorption should be negligible, indicates that any changes in the lattice parameters that would have to be made to account for absorption would be small in comparison to the probable errors quoted.



THE DERIVATION OF A TENTATIVE STRUCTURE AND THE POSSIBLE  
SPACE GROUPS

The  $hk0$  reflections showed a large number of absences, as may be seen on the reciprocal lattice plot in Figure 5. The large number of absences suggested that the sigma crystals might be twinned. A closer examination of the  $hk0$  reflections furthermore revealed the following facts:

(1) Nearly all of the reflections were strong and had intensities that were all about the same, ignoring normal decline. Only a small number of very weak reflections occurred.

(2) All of the strong reflections could be indexed on the basis of two independent pseudo-hexagonal nets with  $a_0$  about  $2.5 \text{ \AA}$ ., slightly distorted to fit the tetragonal cell, and oriented at  $90^\circ$  with respect to one another, there being fifteen lattice points per net within the area covered by the quadratic cross-section of the tetragonal cell. None of the reflections predicted on the basis of these nets <sup>was</sup> were missing. The fit of this layer to two slightly distorted hexagonal nets is shown in Figure 6. It should also be mentioned that:

(3) The reflections that were indexed on the  $l = 1$  layer of the rotation photograph were for the most part uniformly strong reflections having the same values of  $h$  and  $k$  that were observed for the strong reflections on the  $l = 0$  layer, though a few additional very weak reflections were also observed.

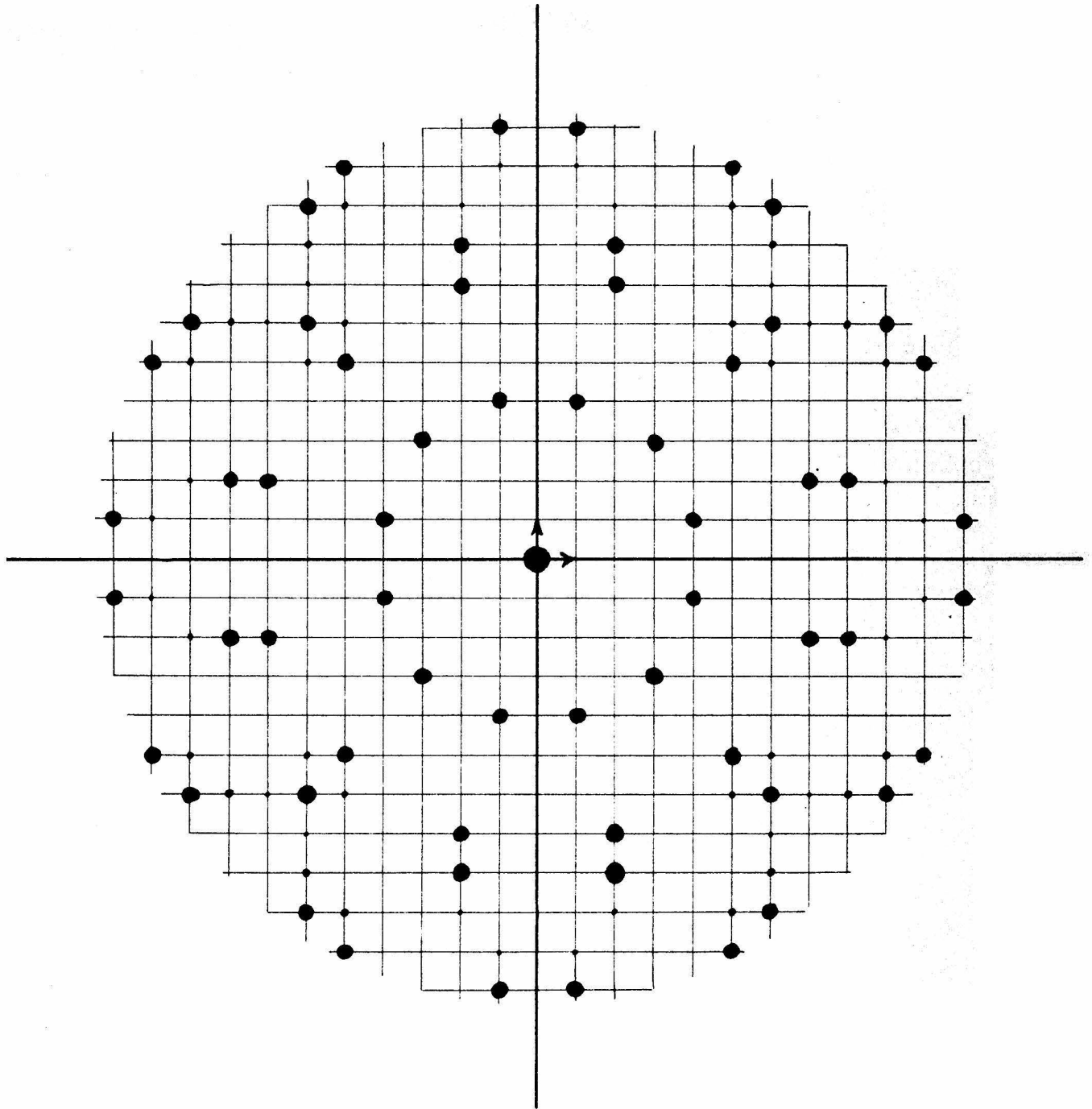


Figure 5. The reciprocal lattice net  $l=0$   
(courtesy Dr. D. P. Shoemaker).

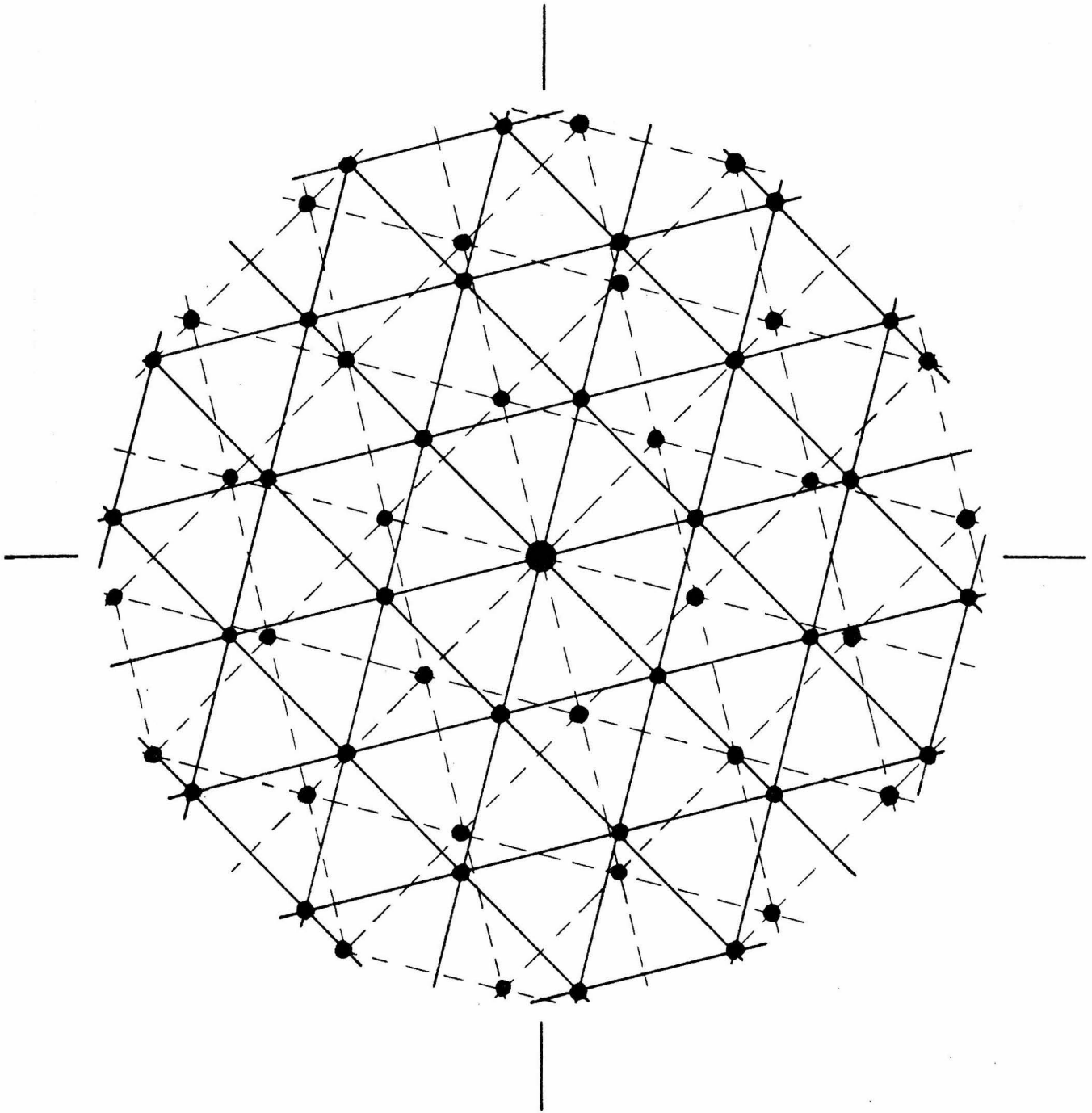


Figure 6. The reciprocal lattice net  $l=0$  with the strong planes fitted to two pseudo-hexagonal nets at  $90^\circ$  to one another (courtesy Dr. D. P. Shoemaker).

These facts, as well as the apparent pseudo-hexagonality revealed by the Laue photograph (Figure 4) taken along the four-fold axis of Crystal No. 6 (showing a gross approximation to an apparent "twelve-fold axis"), could be explained superficially by assuming that the crystal contains twins of two different orientations (at  $90^\circ$  to one another around the c-axis), each twin having a structure (or superstructure) based on a primitive slightly distorted hexagonal lattice (or sublattice) with approximate lattice constants (hexagonal)  $a_0'' = 2.5 \text{ \AA}$ . and  $c_0'' = c_0 = 4.55 \text{ \AA}$ . To account for the uniform intensities it is evident that there can be only one atom per pseudo-hexagonal cell or subcell. However, from the observed density ( $7.600 \text{ g. cm}^{-3}$ , as determined by Duwez and Baen<sup>(3)</sup>), the number of atoms in the tetragonal unit cell is thirty, while the assumptions made above account for only fifteen in an equivalent volume. It is therefore apparent that the structure is not to be sought for in twinning of this kind.

However it occurred to Dr. David Shoemaker that the observed density could be obtained with the assumption of twinning of a different kind; namely, such that the pseudo-hexagonal twins mentioned above interpenetrate, in the sense of occupying the same space. This circumstance would be obtained if the pseudo-hexagonal nets for the two twins alternate, so that the structure consists of alternating pseudo-hexagonal layers  $c_0/2$  apart, each layer being rotated  $90^\circ$

with respect to the adjacent nets through, presumably, the agency of a  $4_2$  screw axis. Each "twin" may be considered as scattering independently for the purpose of this argument, because, inside the limit of the copper data, when the scattering amplitude of one "twin" is finite that of the other "twin" is zero, within the approximation of neglecting the weak reflections. Hence, within this approximation, the reciprocal lattice may be thought of as the superposition of two slightly distorted pseudohexagonal reciprocal lattices oriented at  $90^\circ$  with respect to one another, as appears to fit the observations. The fact that some additional weak reflections are observed might be interpreted to indicate that each "twin" is a superstructure (with the true cell an end-centered orthorhombic pseudohexagonal cell with a volume twice that of the observed tetragonal cell) obtained by deviations of some or all of the atoms from the sublattice points, but since the scattering amplitudes for the weak reflections cannot be considered independently for the two "twins" it appears best to consider the problem of determining atomic positions from the standpoint of the true tetragonal cell and discontinue the use of the concept of separate twins.

From Figure 6 and considerations of tetragonal symmetry it can be seen that the only two possible relative positions of the two pseudohexagonal nets are those indicated by Structure I in Figure 7 and by Structure II in Figure 8.

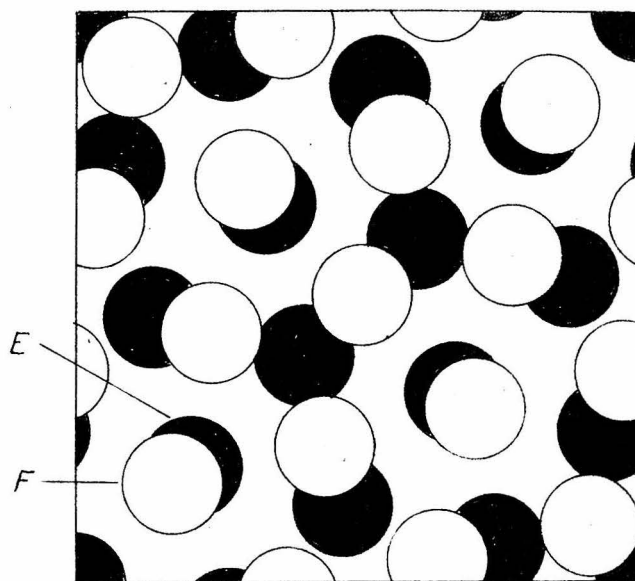


Figure 7. The unit cell of Structure I. Filled circles represent atoms in the plane  $z=0$ ; open circles atoms in the plane  $z=1/2$ .

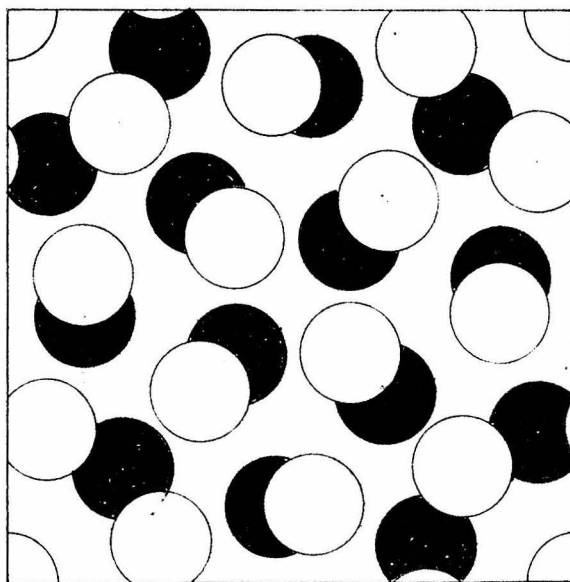


Figure 8. The unit cell of Structure II. Symbols as in Figure 7.

From these figures it is easy to see the extent of the distortion of the nets from hexagonal symmetry. If it is assumed that the distortion is uniform throughout a given net the ratio  $b/a$  (for the orthohexagonal subcell) is  $5/3$  as compared with  $\sqrt{3}$  (1.732) for an undistorted net; that is, the ratio has been decreased by 3.8%.

The problem now presents itself as to which of the two structures shown in Figures 7 and 8 is correct. Structure I has glide planes normal to the  $a$ -axis and the  $b$ -axis but Structure II has no glide planes. Consequently, by Weissenberg photography of the reciprocal lattice layer  $Ok\ell$  it should be possible to select one of the structures as being the correct one. However, in view of the fact that all  $Ok0$  reflections available with copper radiation were too weak to observe, it was considered possible that virtually all  $Ok\ell$  reflections available with copper radiation might be missing, particularly if the structure is an ideal one with all atoms restricted to the planes  $z = 0$  and  $z = \frac{1}{2}$ . In such a case it might be very difficult to determine whether or not the  $n$ -glide planes are present. On the other hand, it will be seen from inspection of the two structures that it should be possible to distinguish between them by considerations of reflections of say the type  $(0.15.l)$ , since it is only at the reciprocal lattice points  $(15m.15n.l)$  that the two pseudohexagonal reciprocal lattice nets coincide point-on-point, so that the scattering amplitudes of both layers

in the unit cell are both finite and have the opportunity to reinforce one another or cancel out. Indeed, the atomic coordinates of both layers in Structure II can be given in integral fifteenths of the cell edge, while in Structure I the atomic coordinates of layer A can be expressed in integral fifteenths (i.e. even thirtieths) while those for layer B are to be expressed in half-integral fifteenths (i.e. odd thirtieths), at least to a good approximation. Hence, if Structure II is correct, (0.15.0) should be observable (with twice the amplitude or four times the intensity of other "ideal" reflections at the same angle) on an (Ok?) Weissenberg photograph taken with molybdenum radiation, and, if the atoms on layer A are restricted to the layer  $z = 0$  and those on layer B to  $z = \frac{1}{2}$ , (0.15.1) should be absent. If Structure I is correct (0.15.0) should be absent (as would be required by an n-glide in any case) and (0.15.1) should be present.

In order to settle the question in the shortest possible time, a Weissenberg photograph was taken with molybdenum radiation of a sufficiently large region of the (Ok?) layer to obtain (0.15.0) and (0.15.1). The photograph showed the former reflection to be absent and the second to be very strong, and therefore confirmed Structure I (Figure 7) as approximately correct (at least in projection) and ruled out Structure II. The fears expressed above regarding the possible absence of all or nearly all (Ok?) reflections within



the copper limit turned out to be unjustified, as reflections of kind other than  $(0.15.l)$  appeared on the film. Those that were observed to be present in this small region of the  $(0kl)$  layer showed n-glide extinctions, and a later  $(0kl)$  photograph taken with copper radiation showed no reflections incompatible with n-glide planes normal to  $a$  and  $b$ .

As among the  $(hk0)$  reflections there were only a few very weak reflections along with the strong ones, and as all the weak reflections had relatively high indices, it was apparent that deviations in the  $x,y$ -plane from the uniform distortion of the hexagonal layers are very small. The  $x$ - and  $y$ -coordinates, when expressed in integral and half-integral fifteenthths of the cell edge, therefore seemed to be quite close to their true values. The fact that the deviations appeared to be very small also made it highly probable that the pseudo-hexagonal layers retained their planarity to a high degree. In fact, a pure layer structure, with atoms restricted to  $z = 0$  and  $z = \frac{1}{2}$ , appeared to be very likely. For such a structure the reciprocal lattice layers with equal to  $0,1,2,3$  etc. would be identical except for the weak reflections and reflections of type  $(15m,15n,l)$ ; all even layers would be identical even in these respects, as would also all odd layers. As was mentioned earlier, the rotation photograph taken with  $c$ -rotation showed a striking similarity between the zeroth and first layer lines. The second layer line however appeared to be different, and later Weissenberg photographs confirmed this. Thus it was apparent that some of the atoms are displaced in the  $c$ -direction by a

considerable distance. On the other hand, it seemed to be very likely that only a small number of atoms had been displaced as otherwise it would be very hard to understand how the "ideal" x,y-projection could be so nearly retained. Therefore, in spite of the different character of the second layer line, it was still considered very likely that the structure was essentially a layer structure with only a few atoms displaced in the c-direction.

In order to determine which of the atoms are displaced from the ideal planes, and to obtain limitations among the possible space groups, intensity data for layers other than  $l = 0$ , including especially  $l = 2$ , were necessary. Weissenberg photographs were therefore taken with  $l$  equal to 1, 2 and 3. When the reciprocal lattice layers were inspected it was found that systematic extinctions occurred only for  $(Ok\bar{l})$  reflections with  $k + l$  odd. These extinctions confirm the presence of n-glides normal to  $\underline{a}$  and  $\underline{b}$ .

Among the space groups that belong to the four crystal classes  $D_{2d}$ ,  $C_{4v}$ ,  $D_4$  and  $D_{4h}$ , compatible with Laue symmetry  $D_{4h}$ , there are three space groups that have the n-glides found in the sigma structure. They are  $D_{2d}^8 - P\bar{4}n2$ ,  $C_{4v}^4 - P4nm$  and  $D_{4h}^{14} - P4/mnm$ . For the ideal layer structure the holohedral space group  $D_{4h}^{14}$  could apply. For any structure derived from it by z-displacements of atoms and no changes in the x and y coordinates, only the space group  $C_{4v}^4$  is possible.

When the plots of the reciprocal lattice layers were compared it was found that:

- (1) The layers  $l = 1$  and  $l = 3$  were almost identical,
- (2) The layer  $l = 0$  was very similar to the layers  $l = 1$  and  $l = 3$  but contained fewer weak reflections, and
- (3) The layer  $l = 2$  was completely different from the other three layers.

These facts, although puzzling at first, very quickly led to a trial structure that provided a very good approximation to the true structure. The fact that the layers  $l = 1$  and  $l = 3$  are almost identical, but at the same time completely different from the layer  $l = 2$ , may be taken as an indication that there is a trend toward periodicity in the reciprocal lattice in the  $c$ -direction, with a repeat of four layers, and with the layers alternating in the fashion ABCBABCBA ..... From this it may be concluded that all atoms in the structure are limited fairly closely to layers  $c_0/4$  apart, so that any atoms displaced from  $z = 0$  and  $z = \frac{1}{2}$  are displaced by about  $c_0/4$ . The fact that layer  $l = 1$  is very similar to  $l = 0$  indicates that only a small number of atoms are displaced in this way. From steric considerations it is apparent that the atoms on layer A ( $z = 0$ ) that are to be displaced to  $z \approx \frac{1}{4}$  must be selected in such a way that the atoms equivalent to them in layer B ( $z = \frac{1}{2}$ ), which are to be moved to  $z \approx \frac{3}{4}$ , lie almost directly above the former in the unit cell.

It turned out to be possible to obtain satisfactory packing (which indeed was much better packing than that in the "ideal" two-layer structure, Structure I), only by displacing the atoms labeled E and F in Figure 7, which have almost the same x- and y-coordinates, and the best result was obtained if the atoms were all displaced in the same direction about one quarter up or down. This is clear since in Structure I these atoms are the centers of hexagons of atoms with the centers almost exactly above each other. In the displaced positions the atoms would be about halfway between two hexagons of atoms. Symmetry considerations made it very likely that in their displaced positions the atoms E and F have exactly the same x,y-coordinates, and the same z-coordinate except for the sign. This is evident as Structure I had mirror planes coinciding with the pseudo-hexagonal nets, and only small changes in the x and y parameters of the displaced atoms (about 1/60) are required to re-establish the mirror planes. The structure derived in this way has space group  $D_{4h}^{14}$  - P4/mmm, and is the trial structure adopted for the subsequent work. More will be said concerning the space group later.

With the notation of the Internationale Tabellen<sup>(14)</sup>, and in terms of space group  $D_{4h}^{14}$ , there are in the unit cell

Atoms of kind A in positions 2(a)

Atoms of kind B in positions 4(f) with  $x = 2/5$

Atoms of kind C in positions 8(i) with  $x = 7/15$  and  
 $y = 2/15$

Atoms of kind D in positions 8(i) with  $x = 11/15$  and  
 $y = 1/15$

Atoms of kind E in positions 8(j) with  $x = 11/60$  and  
 $z = 1/4$

### THE TESTING OF THE TENTATIVE STRUCTURE

After the derivation of the tentative structure the next step was to test the ability of this structure to account for the observed intensities of the reflections. Under the assumption that all atoms had the same form factor, which was very reasonable at this stage since the form factors for iron and chromium are about the same for all Bragg angles, the structure factors were calculated for all reflections of type (hk0), (hkl), (hk2) and (hk3) that are possible with  $\text{CuK}\alpha$  radiation. The form factor was arbitrarily set equal to unity. The results are presented in Table III. In the same table are also presented for comparison, the semi-quantitative values of the observed intensities.

TABLE III

AGREEMENT BETWEEN CALCULATED AND OBSERVED SEMI-QUANTITATIVE  
INTENSITIES

Indices	$\hat{F}$ calc.	Observed intensity	Indices	$\hat{F}$ calc.	Observed intensity
000	30.		002	14.0	
100	0	---	102	0	---
110	- 0.1	---	112	- 2.7	m
200	- 0.1	---	202	10.6	vs
210	- 0.2	---	212	10.7	vs
220	0.0	---	222	- 7.2	s
300	0	---	302	0	---
310	- 0.1	---	312	6.1	ms
320	1.5	---	322	- 2.2	m
400	- 0.1	---	402	1.6	w
410	15.7	vs	412	1.1	w
330	15.6	vs	332	1.1	vw
420	0.6	---	422	- 0.6	---
500	0	---	502	0	---
430	- 0.2	---	432	4.7	m
510	0.6	---	512	- 5.1	mw
520	0.0	---	522	- 6.0	m
440	- 1.3	---	442	- 1.5	---
530	- 1.4	---	532	11.8	s
600	1.2	---	602	-11.7	s
610	0.3	---	612	8.9	ms

TABLE III (continued)

Indices	$\hat{F}$ calc.	Observed intensity	Indices	$\hat{F}$ calc.	Observed intensity
620	- 1.3	---	622	7.3	ms
540	- 1.0	---	542	7.0	ms
630	- 0.8	---	632	- 3.7	m
700	0	---	702	0	---
710	- 0.7	---	712	0.7	---
550	16.0	vs	552	4.0	w
640	0.9	---	642	2.3	vw
720	-16.4	vs	722	- 4.8	m
730	1.0	---	732	- 2.2	---
650	2.4	mw	652	- 2.4	---
800	- 2.6	---	802	13.1	s
810	- 0.8	---	812	2.3	---
740	2.5	---	742	-13.0	s
820	16.6	vs	822	6.1	m
660	15.9	vs	662	5.4	mw
830	1.9	---	832	0.9	---
750	0.8	---	752	3.7	---
840	0.8	---	842	0.9	---
900	0	---	902	0	---
910	0.3	---	912	3.5	w
920	2.8	w	922	- 7.0	mw
760	- 2.4	w	762	6.8	m
850	- 2.2	---	852	- 3.8	w
930	1.5	---	932	- 7.5	ms
940	- 2.8	---	942	10.1	s

TABLE III (continued)

Indices	$\hat{F}$ calc.	Observed Intensity	Indices	$\hat{F}$ calc.	Observed Intensity
770	- 3.3	---	772	- 4.0	---
10.0.0	2.0	---	10.0.2	- 6.0	ms
860	- 3.3	m	862	9.3	ms
10.1.0	3.3	mw	10.1.2	- 9.3	s
10.2.0	- 0.4	---	10.2.2	4.9	m
950	- 3.3	m	952		
10.3.0	- 2.1	---	10.3.2		
870	0.0	---	872		
			10.4.2		
960	15.2	vs	962		
	0		11.0.2		
11.1.0	16.9	vs	11.1.2		
10.5.0	-15.5	vs			
001	0	---	003	0	---
101	0.8	---	103	0.8	---
111	0.6	---	113	0.6	---
201	0	---	203	0	---
211	0.0	---	213	0.0	---
221	- 1.6	---	223	- 1.6	---
301	- 0.8	---	303	- 0.8	---
311	- 2.2	m	313	- 2.2	mw
321	- 0.6	---	323	- 0.6	---
401	0	---	403	0	---
411	13.6	s	413	13.6	s



TABLE III (continued)

Indices	$\hat{F}$ calc.	Observed intensity	Indices	$\hat{F}$ calc.	Observed intensity
331	-13.6	s	333	-13.6	s
421	0.8	---	423	0.8	---
501	- 2.0	---	503	- 2.0	---
431	3.0	m	433	3.0	m
511	3.0	m	513	3.0	w
521	2.2	w	523	2.2	---
441	0.6	---	443	0.6	---
531	0	---	533	0	---
601	0	---	603	0	---
611	1.6	---	613	1.6	---
621	2.2	w	623	2.2	---
541	- 2.2	w	543	- 2.2	w
631	- 3.0	---	633	- 3.0	---
701	5.2	mw	703	5.2	mw
711	- 0.8	---	713	- 0.8	---
551	12.0	s	553	12.0	s
641	- 3.6	w	643	- 3.6	mw
721	11.4	s	723	11.4	s
731	- 1.4	---	733	- 1.4	---
651	0.8	---	653	0.8	---
801	0	---	803	0	---
811	0.0	---	813	0.0	---
741	0.0	---	743	0.0	---
821	10.6	s	823	10.6	s
661	-11.4	s	663	-11.4	s

TABLE III (continued)

Indices	$\hat{F}$ calc.	Observed intensity	Indices	$\hat{F}$ calc.	Observed intensity
831	- 0.6	---	833	- 0.6	---
751	3.0	---	753	3.0	mw
841	5.2	mw	843	5.2	m
901	- 5.2	w	903	- 5.2	m
911	- 3.6	mw	913	- 3.6	mw
921	3.0	m	923	3.0	ms
761	3.0	m	763	3.0	ms
851	2.2	---	853	2.2	vw
931	- 2.2	w	933	- 2.2	mw
941	1.6	---			
771	- 1.6	---			
10.0.1	0	---			
861	- 2.2	m			
10.1.1	- 2.2	m			
10.2.1	3.0	vw			
951	0	---			
10.3.1	5.2	m			
871	- 3.6	m			
961	10.6	s			
11.1.1	- 8.4	s			

-----

vs very strong  
s strong  
ms medium strong  
m medium  
mw medium weak  
w weak  
vw very weak

As the qualitative overall agreement between the observed intensities and the absolute values of the calculated structure factors was excellent, it could not only be concluded that the tentative structure was correct in its main features but also that it was a very good approximation to the true structure so far as the accuracy of atomic positions is concerned. The derivation of the structure up to this point has already been described in the literature by Dr. Shoemaker and the present author<sup>(15)</sup>.

After submitting that paper for publication we learned that Dickins, Douglas and Taylor<sup>(16)</sup> of the Cavendish Laboratory, Cambridge, had, apparently more recently, arrived at essentially the same structure for sigma CoCr as ours for sigma FeCr, except that they tentatively accepted the space group  $C_{4v}^4$ . Both their structure and their space group are based on a comparison of their data with the data obtained for  $\beta$ -uranium by Tucker<sup>(17)</sup>, who has reported for  $\beta$ -uranium essentially the same structure we found for the sigma phase except for the space group (which we believe is probably incorrect). It is interesting to note that although Tucker's data (particularly the (hk0) data) are very similar to ours, he failed to note the superposition of two pseudo-hexagonal nets in the (hk0) layer and arrived at the structure in a much more laborious way by means of a series of Patterson projections and Harker sections.

THE FINAL DETERMINATION OF THE SPACE GROUP

Although it seemed very likely that the true structure has the same space group as the tentative structure - namely  $D_{4h}^{14}$  - the other two space groups,  $C_{4v}^4$  and  $D_{2d}^8$ , were actually still possible, as structures of these symmetries could be generated from the tentative structure even by very small shifts of the atoms, however unlikely small shifts may be in this particular structure. A series of least squares refinements of the parameters, starting from a number of hemihedral structures, might enable the question of the correct space group to be settled if the data were sufficiently good. However it turned out to be possible to settle the question with fair certainty from simpler considerations.

In order to obtain data for the least squares refinement to be carried out later, Weissenberg photographs with  $h$  equal to 0,1,2,3,4 and 5 had been taken as will be described in a later section. The intensities that were obtained confirmed essentially quantitatively the fourfold periodicity (ABCBABCBA.....) of the reciprocal lattice in the  $c$ -direction that has already been referred to. As copper radiation makes available reflections only out to  $l = 5$ , two Weissenberg photographs were taken with molybdenum radiation, one with  $h = 0$  and the other with  $h = 2$ , in order to obtain reflections out to  $l = 12$ . The intensities were not estimated quantitatively, but within the limitations of semi-quantitative comparisons the periodicity was found to hold throughout

these layers; this periodicity also held for non-systematic absences. Incidentally, the  $h = 0$  photograph gave no reflections inconsistent with the  $n$ -glide planes.

Evidently the atoms are very closely confined to layers  $c_0/4$  apart. Any significant deviations of the atomic  $x$ - and  $y$ -coordinates of atoms E from their holohedral relationships would seem to be incompatible with this result from the standpoint of packing, while physical justification for very small  $x$  and  $y$  deviations of atom E does not seem to exist. Much the same can be said regarding removal of the holohedral symmetry by a special ordering of the iron and chromium atoms. Hence the space group  $D_{4h}^{14}$  appears to be almost certainly correct, although the possibility of slight deviations from holohedral symmetry cannot be rigorously ruled out. The only remaining criterion at our disposal is the final agreement between observed structure factors and structure factors calculated for the holohedral structure after refinement. A brief account of the considerations involved in arriving at this conclusion with regard to the space group has been published by the author and Dr. Shoemaker<sup>(18)</sup>. Also given in that article are our reasons for believing that the space group of  $\beta$ -uranium,  $\sigma$ -CoCr, and other sigma phases are probably the holohedral one,  $D_{4h}^{14}$ . The data of Tucker<sup>(17)</sup> on  $\beta$ -uranium were obtained with copper radiation, and hence suffer markedly from absorption; nevertheless, within the apparent precision of the data the periodicity that we have

found in the FeCr data also seems to hold in the  $\beta$ -uranium data, and we doubt if the deviations from the holohedry claimed by Tucker are significant. An (Ok!) Patterson projection calculated by us for his data is very different from the projection published by him and seems to support the holohedry. Since the space group for  $\sigma$ -FeCr is now known to be holohedral with almost complete certainty, and since the evidence that has been presented by Tucker<sup>(17)</sup> for a lower symmetry in  $\beta$ -uranium seems to be erroneous, the presumption of the lower symmetry in  $\sigma$ -CoCr by Dickins, Douglas and Taylor<sup>(16)</sup> is no longer justified and should be replaced in this and all other sigma phases by a presumption of holohedral symmetry until evidence, if any, is obtained to the contrary.

#### THE REFINEMENT OF THE TENTATIVE STRUCTURE

General aspects - As has already been pointed out the structure of the sigma phase could deviate from the tentative structure only very little. It should therefore be feasible to make a least squares refinement of the atomic coordinates immediately without any prior attempts to improve the tentative structure further by trial and error methods.

So far no attempt had been made to determine what kind of atoms are situated in the crystallographically different positions. In the semi-quantitative work done up to this point the small difference between the form factors of iron

and chromium would have made such an attempt out of question. It did not seem very likely that such a determination could be made even by a least squares refinement especially since, for practical reasons, we decided to use  $\text{CuK}\alpha$  radiation in collecting intensity data. Due to the fact that this radiation has a wave length that is not very different from the critical absorption wave lengths of iron and chromium, the small difference in the effective form factors is reduced still further. Nevertheless, we decided to introduce in the least squares refinement not only parameters expressing the positions of the different kinds of atoms but also parameters expressing the effective atomic numbers.

The collection of intensity data - All intensity data were obtained from Weissenberg photographs taken with a Unicam Weissenberg x-ray goniometer having a camera radius of about 30 mm. Nickel filtered  $\text{CuK}\alpha$  radiation was used throughout. Eastman "No Screen" x-ray film was used for all photographs. A multiple film technique was used in which three films were exposed at the same time.

With Crystal No. 4 rotating around the c-axis photographs were taken with  $l = 0, 1, 2$  and  $3$  and with Crystal No. 6 rotating around the a-axis photographs were taken with  $h = 0, 1, 2, 3, 4$  and  $5$ . Due to the small size of crystals rather long exposures were required; they were generally of the order of one hundred hours.

Estimation of intensities - The multiple film technique of de Lange, Robertson and Woodward<sup>(13)</sup> was used. The very

strong intensities were estimated on the film farthest away from the crystal and the very weak reflections on the film closest to the crystal. Intermediate intensities were generally estimated on more than one film. With a knowledge of the film factor (the factor by which the intensity of an x-ray beam is decreased on passing through one film) it was possible to recalculate the intensities so that they were all on the same basis. The most convenient way of estimating intensities was to use intensity strips. The strips used in this work were prepared by exposing repeatedly on the same set of films, at different exposures, the reflection (004) (which is the strongest reflection observable with  $\text{CuK}\alpha$  radiation). Moreover, it was prepared in such a way that the increase in the logarithm of the <sup>exposure</sup>intensity from one spot to the next was constant. For convenience, the intensities were all estimated on a logarithmic scale, with the base of the logarithms set equal to the film factor<sup>(19)</sup>, which for the film used is known to be  $3.7^{(20)}$ . This value was verified in the present work by comparing the three intensity strips that had been prepared simultaneously with the multiple film technique.

In spite of the very small size absorption and/or extinction were sometimes troublesome. It was found that some reflections showed intensities that differed somewhat from the intensities of equivalent reflections observed in other positions on the film. This was apparently due to the irregular shape of the crystal. In such cases the



intensity of the strongest spot was estimated.

Calculations - In view of the fourfold periodicity observed in the reciprocal lattice with increasing  $\lambda$ , it is convenient to combine equivalent layers for the least squares computations. This can be done if the purely geometric part of the structure factor can be dissociated from the atomic form factors. Since iron and chromium have atomic numbers differing only by two, the dependence of the form factors of iron and chromium on scattering angle might be reasonably assumed to be the same. Hence for use in the least squares calculations not only the temperature factor but also the average form factor was divided out of the observed structure factors  $F_{\text{Obs}}$ , giving quantities which will be denoted  $\hat{F}_{\text{Obs}}$ . Likewise, temperature and form factors were left out of the calculation of the corresponding quantities  $\hat{F}_{\text{Calc}}$  from the positional parameters assumed for the tentative structure.

In order to obtain the quantities  $\hat{F}_{\text{Obs}}$  from the intensities estimated visually from the films, the following steps were followed:

(1) Conversion of the intensities from the logarithmic to a linear scale.

(2) Division of the intensities by Lorentz and polarization factors.

(3) Multiplication by suitable empirical exposure constants, one for each set of films, in order to put all intensity values on the same absolute scale.

(4) Averaging of the results obtained for each plane if the intensity was observed on more than one set of films, giving corrected relative intensities  $I'$ .

(5) Division of the square roots of the values  $I'$  by the average atomic form factor for iron and chromium at the corresponding Bragg angles, giving modified relative structure factors called  $\hat{F}'$ .

(6) Division of the  $\hat{F}'$ -values by the combined scale and temperature factors for the corresponding reflections, giving the final modified structure factors  $\hat{F}$  which were used in the least squares refinement. The structure factors calculated in this way should be functions of the positional parameters, the atomic numbers, and the indices only.

Some of the steps have to be explained further. In step 3 the empirical exposure factor was arbitrarily set equal to unity for the reflections observed on the  $l = 2$  Weissenberg photograph. These reflections were selected for the standard exposure scale as they were more numerous than on any other photograph. The exposure factors were then determined for the photographs with  $h$  equal to 0,1,2,3, 4 and 5 by comparing the intensity values for reflections that these photographs had in common with the  $l = 2$  photograph. In a similar way it was possible to determine the exposure factors for the films with  $l$  equal to 0,1 and 3 by comparing intensities for reflections on these films with intensities for the same reflections on the photographs with  $h = 0,1,2$  etc.

In step 6 the combined scale - temperature factors were determined in the following way. If it is assumed that the temperature factor is anisotropic it is reasonable to assume that the scale - temperature factor is a function of the indices  $hkl$  of the type

$$f = C e^{a(h^2 + k^2) + bl^2} \quad \text{eq. 5}$$

or

$$\log_{10} f = \alpha (h^2 + k^2) + \beta l^2 + \gamma$$

where  $C$ ,  $a$ ,  $b$ ,  $\alpha$ ,  $\beta$  and  $\gamma$  are constants. The scale factor is naturally equal to  $C$  or  $\text{antilog } \gamma$ . The problem at hand is to determine the constants  $\alpha$ ,  $\beta$  and  $\gamma$ . Now we can write

$$f \sim \frac{\hat{F}'}{\hat{F}_{\text{calc}}}$$

if  $\hat{F}_{\text{calc}}$  is based on a set of reasonably correct parameters, such as the trial parameters already given. We had already evaluated  $\hat{F}_{\text{calc}}$  on the basis of these parameters (see Table III). The constants  $\alpha$ ,  $\beta$  and  $\gamma$  could then be calculated by the least-squares solution of a set of observational equations of the type

$$\log \frac{\hat{F}'}{\hat{F}_{\text{calc}}} = \alpha (h^2 + k^2) + \beta l^2 + \gamma \quad \text{eq. 6}$$

Only equations corresponding to reflections with large  $\hat{F}_{\text{calc}}$  values were used, since nearly all of the reflections were either strong or weak, and the weak reflections would have

had small weight. The result of the calculations was

$$\log_{10} f = 0.0016(h^2 + k^2) + 0.0055l^2 - 1.134 \quad \text{eq. 7}$$

Since  $f$  is increasing with increasing values of  $h$ ,  $k$ , and  $l$  an absorption effect may be present in addition to the temperature effect. As furthermore

$$\frac{0.0016}{0.0055} \sim \frac{c_0^2}{a_0^2}$$

where  $a_0$  and  $c_0$  are the unit cell dimensions, the combined scale-temperature factor is approximately isotropic.

The calculations of the  $\hat{F}_{\text{calc}}$  and of the partial derivatives  $\frac{\partial \hat{F}}{\partial x_k}$  for use in the least squares treatment were done with the help of the general expression for the geometric structure factor given in the Internationale Tabellen<sup>(14)</sup>. The contribution  $A$  to the structure factor from sixteen equivalent atoms in general positions is, according to this reference,

$$A = 8 \cos 2\pi lz \left[ \cos 2\pi \left( hx - \frac{h+k+l}{4} \right) \cos 2\pi \left( ky + \frac{h+k+l}{4} \right) + \cos 2\pi \left( kx + \frac{h+k+l}{4} \right) \cos 2\pi \left( hy - \frac{h+k+l}{4} \right) \right] \quad \text{eq. 8}$$

For the purpose of introducing an atomic number parameter the right hand side of Equation 8 may be multiplied by  $Z/Z_0$  or  $R$ .

The least squares treatment was carried out in accordance with the procedure given by Hughes<sup>(21)</sup>, except with regard to the weighting. However, instead of refining all positional parameters simultaneously, it was found convenient, in view of the fourfold periodicity of the reciprocal lattice already referred to, to refine the one  $z$ -parameter (for atoms E) separately and to combine the essentially equivalent reciprocal lattice nets for the purpose of reducing the number of observational equations needed for the refinement of the  $x$  and  $y$  parameters. This procedure would be equivalent to the complete least squares refinement if in the latter the off-diagonal matrix elements connecting the  $z$  parameter with the  $x$  and  $y$  parameters and the atomic number parameters were neglected.

For the refinement of the one  $z$  parameter, Equation 8 may be written

$$A = G(x,y,R)\cos 2\pi lz$$

If we take the partial derivative with respect to  $z$  we get

$$\frac{\partial A}{\partial z} = -G(x,y,R) 2\pi l \sin 2\pi lz$$

For  $l$  even and  $z = \frac{1}{4}$  this expression vanishes. For  $l$  odd and  $z = \frac{1}{4}$  we obtain

$$\frac{\partial A}{\partial z} = \pm 2\pi l G(x,y,R) \quad - \text{ for } l=1,5,9 \text{ and } + \text{ for } l=3,7,11..$$

Consequently for small z-shifts of atoms E the structure factor will change by an amount that is proportional to  $l$ . This makes it possible to determine the deviation of the z-coordinate of atoms E from the approximate value of  $\frac{1}{4}$  by means of a simple least squares calculation using the differences among the  $\hat{F}_{\text{Obs}}$ -values for reflections with the same h and k indices and  $l$  equal to 1,3,5 etc.

The weights  $w$  for all reflections were determined by the following procedure. The weight  $w$  of an observed quantity  $\hat{F}_{\text{Obs}}$  can be written

$$w = \frac{1}{\sigma_{\hat{F}}^2} \quad \text{eq. 9}$$

where  $\sigma_{\hat{F}}$  is the standard deviation. The standard deviations of the quantities  $\hat{F}_{\text{Obs}}$  consequently had to be determined. The standard deviations in the corrected relative intensities  $I'$ , in all cases where  $I'$  represented the average of values obtained on two or three photographs, were calculated from the deviations of the individual values from the means. These standard deviations were divided by the respective  $I'$  values, and then by two to obtain relative standard deviations in the structure factors. These relative standard deviations were plotted against the uncorrected intensities as obtained directly from the photographs. A smooth curve was then drawn through the field of rather scattered points to represent the average relative standard deviation  $\sigma_{\hat{F}}/\hat{F}$  as a function of the uncorrected, directly observed intensity.

This curve showed that  $\sigma_{\hat{F}}/\hat{F}$  is smaller for medium-strong reflections than for either strong or weak reflections. From this curve the relative standard deviations were obtained for all observed reflections. In each case where a given plane had been measured two or three times, the value read from the curve was divided by the square root of the number of observations. Multiplication of these values by the  $\hat{F}$  gave the standard deviations required in Equation 9.

The procedure just described was applicable to observed reflections. However, as has been mentioned before a great number of non-systematic extinctions were observed among reflections with  $l = 0, 1, 3, 4, 5, \dots$ . These pseudo-absences certainly should be considered in the refinement of the structural parameters. This was done as follows. Only reflections with an uncorrected intensity greater than a certain minimum could be observed on the photographs. From this minimum value it was possible to determine for each unobserved plane the value of  $\hat{F}$  which corresponds to the smallest observable intensity; this value of  $\hat{F}$  may be denoted  $\hat{F}_{\min}$ . Now for an unobserved reflection  $\hat{F}_{\text{obs}}$  may have any value satisfying the inequalities

$$-\hat{F}_{\min} < \hat{F}_{\text{obs}} < + \hat{F}_{\min}$$

It may be assumed that any value within these limits is about equally probable, leading to an expectation value of

$\hat{F}_{\text{obs}}$  equal to zero. Consequently, an observational equation can be written for such a reflection, in which  $\hat{F}_{\text{obs}}$  is set equal to zero. The normalized probability distribution function of  $\hat{F}_{\text{obs}}$  is

$$P(\hat{F}_{\text{obs}}) = \frac{1}{2\hat{F}_{\text{min}}}$$

We can now express the standard deviation of  $\hat{F}_{\text{obs}}$  from its expectation value zero by the equation

$$\sigma_{\hat{F}}^2 = \overline{(\hat{F}_{\text{obs}} - \hat{F}_{\text{exp}})^2} = \overline{\hat{F}_{\text{obs}}^2}$$

or

$$\sigma_{\hat{F}}^2 = \int_{-\hat{F}_{\text{min}}}^{+\hat{F}_{\text{min}}} P(\hat{F}) \hat{F}^2 d\hat{F} = \frac{\hat{F}_{\text{min}}^2}{3}$$

The weight  $w$  consequently is

$$w = \frac{3}{\hat{F}_{\text{min}}^2}$$

There was a total of 179 different reflections. The corresponding weights varied from 1 to 516. There were 87 weights smaller than 10 and 75 smaller than 5. The average of the weights larger than 10 was of the order 100. To reduce the amount of work in the least squares calculation it was decided that all observational equations of a weight smaller than 10 should be excluded. The least squares refinement was consequently based on 92 different reflections. It should be mentioned that all the observational equations for the



non-systematic extinctions were excluded in this way; the maximum weight for such an observational equation being three.

With these weights the refinement of the  $z$  parameter was first carried out. Then, for the purpose of refining the remaining parameters, the value of  $\hat{F}_{\text{obs}}$  for each plane with  $l = 0$  was averaged with that for the corresponding plane with  $l = 4$ , and the weights were added. Likewise corresponding values of  $\hat{F}$  for  $l = 1, 3$ , and  $5$  were averaged and their weights added. The calculations were carried out from this point in the usual way, the computation of the matrix elements (including all off-diagonal matrix elements) being carried out by means of punched cards and IBM machines. The normal equations were solved by an iteration procedure for two cases: (1) for all parameters, with the complete matrix; and (2) for the positional parameters alone, matrix elements connecting these with the atomic number parameters being omitted. The object of carrying out the calculation for the second case was to avoid additional errors due to the inclusion of superfluous parameters in case the so-called atomic number parameters proved incapable of satisfactory interpretation.

The results of the refinement of parameters - The results of the least squares refinement of all positional and atomic number parameters are presented in Table IV. The uncertainties quoted are probable errors.

TABLE IV

RESULTS OF REFINEMENT OF ALL STRUCTURAL PARAMETERS

Kind of atoms	Empirical atomic no.	x	y	z
A, in 2(a)	27.5 $\pm$ 0.8	0.	0	0
B, in 4(f)	23.3 $\pm$ 0.5	0.3976 $\pm$ 0.0005	0.3976 $\pm$ 0.0005	0
C, in 8(i)	25.2 $\pm$ 0.4	0.4624 $\pm$ 0.0006	0.1322 $\pm$ 0.0005	0
D, in 8(i)	25.2 $\pm$ 0.4	0.7374 $\pm$ 0.0005	0.0651 $\pm$ 0.0005	0
E, in 8(j)	22.8 $\pm$ 0.4	0.1824 $\pm$ 0.0005	0.1824 $\pm$ 0.0005	0.2524 $\pm$ 0.0006

-----

The weighted average of the empirical atomic numbers of all the atoms is 24.5 as compared to 25 which is the expected average. The difference may be due to an incorrect scale factor.

-----

The results of the refinement of the positional parameters alone are presented in Table V.

TABLE V

RESULTS OF REFINEMENT OF POSITIONAL PARAMETERS ALONE

Kind of atoms	x	y	z
A, in 2(a)	0	0	0
B, in 4(f)	0.3981 $\pm$ 0.0006	0.3981 $\pm$ 0.0006	0
C, in 8(i)	0.4632 $\pm$ 0.0007	0.1316 $\pm$ 0.0006	0
D, in 8(i)	0.7376 $\pm$ 0.0006	0.0653 $\pm$ 0.0006	0
E, in 8(j)	0.1823 $\pm$ 0.0006	0.1823 $\pm$ 0.0006	0.2524 $\pm$ 0.0006

It is seen that the second set of positional parameters is practically identical with the first set.

In Table VI the calculated and observed structure factors are presented for all reflections except a few weak ones at large Bragg angles, for which no quantitative measurements were made as the intensity could not be measured with satisfactory accuracy. The structure factors were calculated on the basis of the parameters in Table IV.

While it thus may be said that the crystal structure of the sigma phase is now known with sufficient accuracy so far as the positions of the atoms are concerned, this is not the case with regard to identification of the atoms with respect to kind. The atomic number parameters in Table IV seem to indicate that a differentiation as to kind actually takes place but the results can not be interpreted unambiguously. Some reasonable interpretations of the atomic numbers can be made after the coordination of the different atoms has been investigated. This will be described later.

TABLE VI

## OBSERVED AND CALCULATED STRUCTURE FACTORS

Indices	$\hat{F}_{\text{obs}}$	$\hat{F}_{\text{calc}}$	Indices	$\hat{F}_{\text{obs}}$	$\hat{F}_{\text{calc}}$	Indices	$\hat{F}_{\text{obs}}$	$\hat{F}_{\text{calc}}$
000			002	14.8	14.8	004	30.6	29.4
100		0	102		0	104		0
110	< 1.0	-0.1	112	2.0	-0.5	114	< 1.0	-0.1
200	< 1.0	0.4	202	11.1	10.1	204	< 1.0	0.4
210	< 1.0	0.3	212	11.8	10.3	214	< 1.0	0.3
220	< 1.0	-0.4	222	9.7	-6.9	224	< 1.0	-0.4
300		0	302		0	304		0
310	< 1.0	0.1	312	5.8	5.9	314	< 1.0	0.1
320	< 1.4	1.0	322	3.4	-2.2	324	< 1.4	1.0
400	< 1.0	0.0	402	2.2	2.0	404	< 1.0	0.0
410	14.4	15.0	412	2.9	1.7	414	16.1	15.0
330	13.8	14.8	332	< 1.7	1.5	334	16.2	14.8
420	< 1.5	1.1	422	< 1.5	-0.2	424	< 1.5	1.1
500		0	502		0	504		0
430	< 1.0	-0.5	432	4.4	3.7	434	< 1.0	-0.5
510	< 1.5	1.6	512	3.7	-3.7	514	< 1.5	1.6
520	< 1.0	-0.5	522	6.9	-6.4	524	< 1.0	-0.5
440	< 1.5	-0.2	442	< 2.0	-0.5	444	< 1.5	-0.2
530	< 1.5	-0.6	532	13.4	11.4	534	< 1.5	-0.6
600	1.5	0.5	602	12.4	-11.7	604	< 1.5	0.5
610	< 1.5	1.5	612	7.3	8.9	614	< 1.5	1.5
620	< 1.7	1.0	622	7.9	7.0	624	< 1.7	1.0
540	< 1.7	-1.2	542	7.6	6.5	544	< 1.7	-1.2
630	< 1.7	-0.5	632	3.3	2.8	634	< 1.7	-0.5

TABLE VI (Continued)

Indices	$\hat{F}_{obs}$	$\hat{F}_{calc}$	Indices	$\hat{F}_{obs}$	$\hat{F}_{calc}$	Indices	$\hat{F}_{obs}$	$\hat{F}_{calc}$
700		0	702		0	704		0
710	< 1.7	0.2	712	< 2.5	1.2	714	< 1.7	0.2
550	11.8	14.3	552	3.9	3.8	554	15.3	14.3
640	< 1.8	1.0	642	2.9	2.7	644	< 1.8	1.0
720	16.7	-16.6	722	6.5	-5.8	724	-15.2	-16.6
730	< 1.8	0.5	732	< 2.0	-1.8	734	< 1.8	0.5
650	3.4	3.3	652	< 2.0	-1.1	654	3.6	3.3
800	1.8	-1.4	802	13.1	12.7	804	< 1.8	-1.4
810	< 1.8	-0.8	812	< 2.1	2.7	814	< 1.8	-0.8
740	< 2.0	1.3	742	13.5	-12.9	744	< 2.0	1.3
820	16.5	17.1	822	7.9	7.7			
660	14.8	15.3	662	4.5	5.2			
830	< 2.0	1.6	832	< 2.0	0.5			
750	< 2.0	0.8	752	3.4	3.0			
840	< 2.0	1.1	842	< 1.9	0.9			
900		0	902		0			
910	< 2.1	1.3	912	4.3	4.5			
920	3.1	3.6	922	5.9	-5.1			
760	2.1	-2.2	762	5.2	5.8			
850	2.1	-1.7	852	4.3	-3.6			
930	< 2.1	0.8	932	6.5	-8.1			
940	< 2.1	-0.3	942	10.9	10.9			
770	< 2.0	-1.1	772	< 1.8	-1.5			
10.0.0	< 1.9	0.8	10.0.2	6.3	-5.7			
860	3.4	-3.6	862	5.4	8.1			

TABLE VI (continued)

Indices	$\hat{F}_{obs}$	$\hat{F}_{calc}$	Indices	$\hat{F}_{obs}$	$\hat{F}_{calc}$	Indices	$\hat{F}_{obs}$	$\hat{F}_{calc}$
10.1.0	3.0	3.2	10.1.2	7.8	-8.7			
10.2.0	<1.9	0.2	10.2.2	4.2	4.4			
950	3.9	-4.2						
10.3.0	<1.9	-1.4						
870	<1.8	-0.5						
960	10.4	14.6						
11.1.0	12.5	16.5						
10.5.0	10.8	-15.0						
001		0	003		0	005		0
101*		1.4	103*		1.6	105*		1.2
111	<1.0	0.5	113	<1.0	0.1	115	<1.0	1.0
201		0	203		0	205		0
211	<1.3	0.3	213	<1.3	0.2	215	<1.3	0.4
221	<1.6	-0.6	223	<1.6	-1.0	225	<1.6	-0.3
301	<1.6	-0.3	303	<1.6	-0.8	305	<1.6	0.1
311	2.7	-2.3	313	2.6	-2.1	315	2.6	-2.5
321	<1.6	-0.8	323	<1.6	-0.5	325	<1.6	-1.2
401		0	403		0	405		0
411	12.8	13.8	413	13.1	13.8	415	12.4	13.8
331	14.7	-13.8	333	14.8	-13.9	335	13.9	-13.8
421	<2.2	1.3	423	<2.2	1.6	425	<2.2	0.7
501	<1.7	-1.3	503	<1.7	-0.9	505	<1.7	-1.7
431	3.8	3.5	433	3.8	3.5	435	3.1	3.4
511	3.3	3.2	513	3.6	3.4	515	3.0	3.0

TABLE VI (continued)

Indices	$\hat{F}_{obs}$	$\hat{F}_{calc}$	Indices	$\hat{F}_{obs}$	$\hat{F}_{calc}$	Indices	$\hat{F}_{obs}$	$\hat{F}_{calc}$
521	2.9	2.3	523	3.0	2.0	525	2.8	2.5
441	< 2.5	0.3	443	< 2.5	-0.2			
531	< 2.5	0.0	533	< 2.5	-0.1			
601		0	603		0			
611	< 2.0	0.7	613	< 2.0	0.8			
621	3.4	2.9	623	observed	2.7			
541	3.2	-2.3	543	3.2	-2.4			
631	< 2.2	-2.0	633	< 2.2	-2.4			
701	4.4	5.2	703	4.4	5.0			
711	< 2.5	-0.6	713	< 2.5	-1.0			
551	13.4	13.1	553	14.3	13.0			
641	3.5	-3.7	643	4.0	-3.4			
721	11.8	10.8	723	10.3	10.9			
731	< 2.3	-2.3	733	< 2.3	-2.1			
651	< 2.0	1.5	653	< 2.0	1.9			
801		0	803		0			
811	< 1.9	-0.2	813	< 1.9	-0.4			
741	< 1.8	-0.4	743	< 1.8	-0.4			
821	10.5	9.7	823	8.1	9.6			
661	9.7	-11.9	663	11.2	-12.0			
831	< 1.7	0.9	833	< 1.7	1.5			
751	2.6	-3.3	753	3.3	-3.1			
841	4.6	4.5	843	4.4	4.7			
901	3.2	-3.6	903	3.6	-3.8			

TABLE VI (continued)

Indices	$\hat{F}_{obs}$	$\hat{F}_{calc}$	Indices	$\hat{F}_{obs}$	$\hat{F}_{calc}$	Indices	$\hat{F}_{obs}$	$\hat{F}_{calc}$
911	3.5	-3.2	913	2.5	-2.7			
921	4.2	3.9	923	3.9	4.1			
761	4.3	4.2	763	3.9	4.2			
851	observed	3.1	853	observed	2.7			
931	3.3	-2.5	933	2.4	-2.6			
941	< 1.6	0.6						
771	< 1.7	-1.7						
10.0.1		0						
861	3.6	-2.8						
10.1.1	3.6	-3.5						
10.2.1	2.4	2.3						
951	< 1.7	0.2						
10.3.1	4.3	5.7						
871	3.1	-3.6						
961	8.3	10.9						
11.1.1	6.5	-8.6						

-----  
\* The geometry of the camera did not allow these spots to be observed.



DISCUSSION OF THE STRUCTURE

General remarks

The final structure, as obtained by least squares refinement, is shown in Figure 9. The space group is almost certainly  $D_{4h}^{14}$  - P4/mmm. The parameters that have been used in the calculation of the final structure factors (Table VI) are those given in Table IV; the parameters that have been used for computation of interatomic distances later on are those given in Table V because of lack of an unambiguous interpretation of the atomic number parameters.

The packing is very novel and interesting; it might even be given the name "tetragonal closest packing", for a density which is about the average of that of iron and chromium in the close-packed elementary states is achieved, though of course the conventional use of the term "closest packing" is restricted to simple structures in which all atoms are equivalent. The structure may be described as consisting of hexagonal close-packed layers which are locked together by atoms displaced from these layers to positions about half-way between them. It is easy to see why the sigma phases are hard, brittle substances, as there exist no clearly apparent slip planes.

The coordination polyhedra and interatomic distances - The following coordination polyhedra, always of course with a certain degree of distortion, were found to occur in the sigma structure:

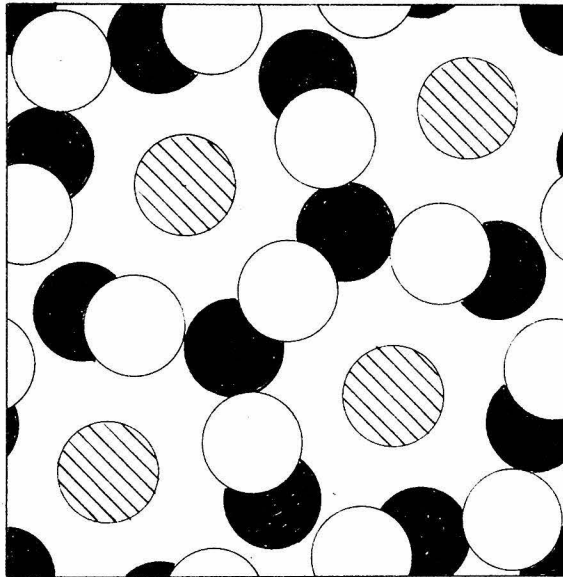


Figure 9. The unit cell of  $\sigma$ -FeCr. Filled and open circles represent atoms in the planes  $z = 0$  and  $z = 1/2$  respectively, while shaded circles each represent two atoms above one another with  $z$ -coordinates equal to approximately  $1/4$  and  $3/4$  respectively.

(1) The regular icosahedron, with coordination number 12: Atoms of kind A and D;

(2) A sexi-icosahedron, with coordination number 15: Atoms of kind B; and

(3) A tetra-icosahedron with coordination number 14: Atoms of kind C and E.

All three polyhedra are built up exclusively with triangular faces. Of the polyhedra only the icosahedron is regular. The tetra-icosahedron, which has twenty-four faces, is obtained from the icosahedron by changing one of the five-fold axis to a six-fold axis. It has point symmetry,  $D_{6d}$ . It is far from approximately spherical, being flattened (oblate) along the six-fold axis. The sexi-icosahedron, which has twenty-six faces, is obtained from the tetra-icosahedron by replacing one of its six-fold vertices by two vertices, which then become five-fold, and distorting the polyhedron so that all its edges become approximately equal and a polyhedron of point symmetry  $D_{3h}$  results. This polyhedron is somewhat extended (prolate) along the three-fold axis. The polyhedra as they occur in the sigma structure are naturally all distorted so that the point symmetries given above are destroyed.

The interatomic distances, with the number of times they appear for each atom, are given in Table VII.

TABLE VII

INTERATOMIC DISTANCES

A - B	4	2.603 A	B - A	2	2.603 A	C - B	1	2.414 A
A - D	4	2.380 A	B - B	1	2.536 A	C - C	1	2.404 A
A - E	$\frac{4}{12}$	2.542 A	B - C	2	2.414 A	C - C	4	2.838 A
			B - D	4	2.695 A	C - D	1	2.483 A
			B - E	4	2.833 A	C - D	1	2.476 A
			B - E	$\frac{2}{15}$	2.920 A	C - D	2	2.470 A
						C - E	2	2.763 A
						C - E	$\frac{2}{14}$	2.768 A
			D - A	1	2.380 A	E - A	1	2.542 A
			D - B	2	2.695 A	E - B	1	2.920 A
			D - C	1	2.483 A	E - B	2	2.833 A
			D - C	1	2.476 A	E - C	2	2.763 A
			D - C	2	2.470 A	E - C	2	2.768 A
			D - D	1	2.453 A	E - D	2	2.538 A
			D - E	2	2.538 A	E - D	2	2.562 A
			D - E	$\frac{2}{12}$	2.562 A	E - E	1	2.253 A
						E - E	$\frac{1}{14}$	2.294 A

It may be noted that a few distances, e.g. the distance B - E, are remarkably long, so long in fact that one might doubt that the atom E belongs to the coordination polyhedron surrounding atom B as a ligate to this atom. But when it is considered that the interatomic distances are distributed fairly evenly over a range from 2.25 Å to 2.92 Å it is hard to exclude some atoms as being non-ligates. The very short E - E bond actually is as remarkable as the long bonds. One might think that these short bonds are single bonds or even bonds with bond numbers exceeding one, but it seems also possible that they are bonds of high d-character or even bonds of lower order that have been compressed due to lack of space for the atoms. It therefore seems very likely that all the atoms in the coordination shells are ligates of the central atom with bonds that may very well be of widely different orders. These bond orders will be discussed in detail later. It is an interesting fact that in the sigma phase one kind of atoms, kind B, has coordination number fifteen which is not found very often.

It is interesting to note that the sigma phase structure is related to the gamma brass structure in that the icosahedral coordination also occurs for all atoms in gamma brass.

The possible ordering of the iron and chromium atoms - As has been mentioned earlier it is hardly possible to draw any very reliable conclusions as to ordering of the iron and chromium atoms in the sigma structure from the results presented in Table IV. The fact that the atomic numbers turned

out to be different might for example be due to the fact that the atomic form factors may be considerably different at large Bragg angles as a result of different types of coordination. It is therefore not impossible that the iron and chromium atoms are distributed with complete randomness in the structure.

It is rather likely however that at least some ordering actually occurs in the structure in view of the highly different coordination polyhedra that exist, and also in view of the fact that the sigma phase occurs in binary systems like the iron-molybdenum system. The difference between the metallic radii for these two metals is so great that a random ordering seems unlikely. Attempts were therefore made to interpret the results in Table IV, as indicating an ordered structure.

(a) The simplest interpretation is clearly that atoms A are of one kind (presumably iron), atoms B and E of the other kind (chromium), and atoms C and D intermediate (random occupancy of the two kinds). This would lead to a ratio between the number of iron atoms and the number of chromium atoms of 1:2 whereas the actual ratio appears to be in the neighborhood of 1:1. Consequently this interpretation, although not impossible in modified form, does not seem very attractive, particularly since it provides no very satisfactory correlation with coordination.

(b) The empirical atomic number of atoms A (27.5) is much higher than that of the others; it is reasonable to assume these atoms to be iron. Their coordination polyhedron

is the icosahedron. Atoms D have the same coordination polyhedron and the atomic number 25.2, which is 2.3 (or about 2) smaller than that of atoms A; they may reasonably be assumed to be chromium atoms. The atoms E have such a small empirical atomic number (22.8) that it is almost necessary to assume them to be chromium atoms; the decrease from 25.2 might be ascribable to the difference in coordination. If we then assume that the tetra-icosahedral coordination decreases the effective atomic number we have to conclude that the atoms C, which have the same coordination polyhedron as the atoms E, may be iron atoms, since the difference between the atomic numbers of atoms C and E is 2.4 or about 2. To obtain a structure of an approximately correct composition (46.7 at. % Cr), it is then necessary to assume atoms B to be iron atoms. This is consistent with the trend already observed, for the empirical atomic numbers of iron atoms A and C show a decrease with increasing coordination number. The structure obtained in this way would contain 53.3 at. % chromium.

(c) Dr. Shoemaker has suggested an assignment on quite different considerations. As was mentioned in the introduction to this thesis Professor Pol Duwez has pointed out that in all known sigma phase binary compounds one of the two constituents has the A1 structure as one of its allotropic modifications in the elementary state, while the other has the A2 structure as one of its allotropic modifications. In

the FeCr-system the one with the A1 structure would be iron and the one with the A2 structure would be chromium. It is then reasonable to place the iron atoms in positions of ligancy twelve and the chromium atoms in positions of ligancy fourteen. Atoms A and D have coordination number twelve and are therefore well suited to iron. Atoms C and E have coordination number fourteen and are therefore suited to chromium. As some of the distances between these atoms and the atoms in the coordination shells are quite long (2.8 and 2.9 Å) it is possible that the effective number of ligates is twelve or thirteen instead of fourteen. There may, therefore, be some random replacement of chromium by iron. Atoms B have coordination number fifteen. The six distances to the atoms of kind E are however so long that it might be appropriate to consider the three pairs of atoms of kind E as equivalent to three single atoms, so as to give an effective ligancy of twelve. The atoms B may therefore be either iron or chromium, perhaps randomly. If we assume that positions A and D are occupied by iron atoms, positions B by iron and chromium in about equal proportions, and positions C and E by chromium and iron in the ratio three to one, we obtain a structure of the composition Fe<sub>8</sub>Cr<sub>7</sub> that has a chromium content of 46.7 at.%. This composition corresponds to the peak of the sigma region in the phase diagram. It will be observed that this assignment bears no obvious relation to the empirical atomic number parameters.



These three postulated assignments may be considered in the light of the valences of the various atoms, as calculated from their bond numbers by use of the equation due to Professor Pauling<sup>(22)</sup>,

$$D(n) = D(1) - 0.600 \log_{10} n$$

and the single-bond radii given by Professor Pauling for iron and chromium<sup>(23)</sup> (1.165 and 1.176 respectively). Since these two radii are very nearly the same, their average was taken for all calculations. The valences obtained in this way are shown in Table VIII. The results are approximate, for no allowance was made for the possibility of different d-characters in the various bonds. The two very short bond distances for atoms E lead to bond numbers of 1.4 and 1.2; these are quite possibly single bonds with large d-characters. However, for the purpose of calculating approximate valences it might well be justifiable to assume that differences in d-character will largely cancel each other out when the bond numbers are summed over all ligates. Also presented in Table VIII are the three postulated assignments discussed above.

TABLE VIII

APPROXIMATE EMPIRICAL VALENCES AND POSTULATED  
ORDERING ASSIGNMENTS

Atom	Empir. at.No.	Coord. number	Valence	Assignment (a)*	Assignment (b)	Assignment (c)
A	27.5	12	6.76	Fe	Fe	Fe
B	23.3	15	4.55	Cr	Fe	Fe,Cr 1:1
C	25.2	14	5.34	Fe,Cr	Fe	Fe,Cr 1:3
D	25.2	12	6.23	Fe,Cr	Cr	Fe
E	22.8	12	6.07	Cr	Cr	Fe,Cr 1:3

-----  
\* There is presumed to be enough replacement of Cr by Fe to obtain the actual composition.

There seems to be no obvious correlation between the valences and the assignment (b). With assignments (a) and (c) the valence of 4.55 found for atoms B could be considered to be the result of the presence of trivalent chromium and 5.78-valent iron; all other positions can be filled by either iron or hexivalent chromium without much change in the normal valences, in view of the approximate nature of the empirical valences. With assignment (c) the 1:1 mixture of trivalent chromium and 5.78-valent iron predicts an average valence of 4.39, in close agreement with the value 4.55 found for atoms B.

There seems to be no clear cut case for any of these three assignments, and the results of these considerations of ordering in the sigma phase must be regarded as indecisive. An investigation of the sigma phase FeMo is in progress, and results obtained to date are described in a later section. It is hoped that reliable information regarding the ordering in this phase can be obtained, and the large difference in form factors gives good promise of making this possible. However, in view of the atomic size factor, it is by no means certain that the results obtained for the preferred positions of molybdenum in sigma-FeMo will be applicable to chromium in sigma-FeCr.

BRILLOUIN ZONE STABILIZATION

For a number of intermetallic compounds such as the gamma alloys and alpha manganese it has been found that a well marked Brillouin polyhedron occurs that contains only slightly more than enough states to accommodate all the valence electrons<sup>(24)</sup>. It is likely that in these cases the filled Brillouin polyhedron contributes to the stability of the structure.

Dr. Shoemaker undertook to investigate the question as to whether or not Brillouin zone stabilization occurs also in the sigma structure. He found one inner polyhedron formed by planes correspond to (330), (410), (331), (411), (202), (212), (222) and (002) that contains enough states for 1.4 electrons per atom. Dr. Shoemaker also found an outer very strongly marked polyhedron formed by planes corresponding to (720), (550), (721), (551), (602), (532), (413), (333) and (004). This polyhedron is shown in Figure 10. It contains enough quantum states to accommodate 6.97 electrons per atom. This is of considerable interest, for valences greater than six have been observed very rarely, if ever, in metals; indeed it is likely that any increase in valence beyond six provides no significant increase in orbital strength<sup>(25)</sup>. However, the number of electrons beyond the filled argon shell is eight for iron and six for chromium which could give at most an average of seven electrons per atom for a compound of the composition FeCr, which

-85a-

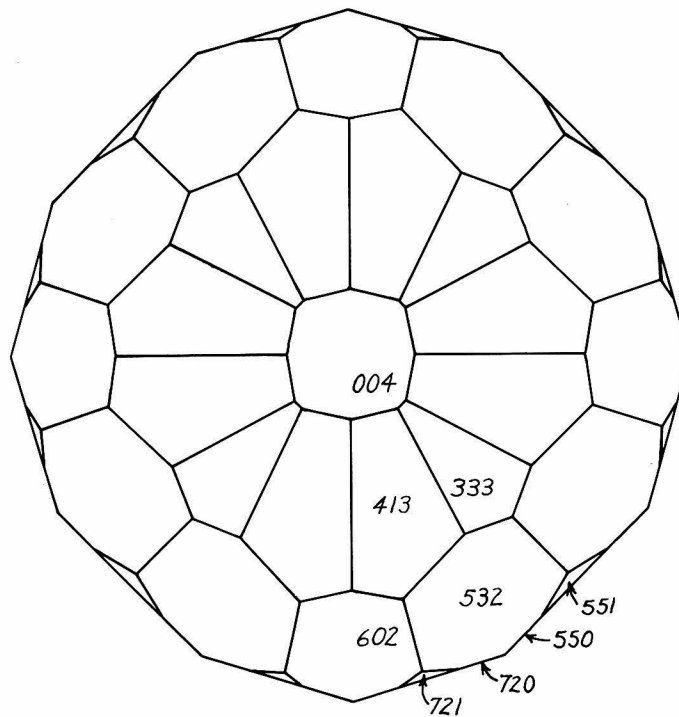
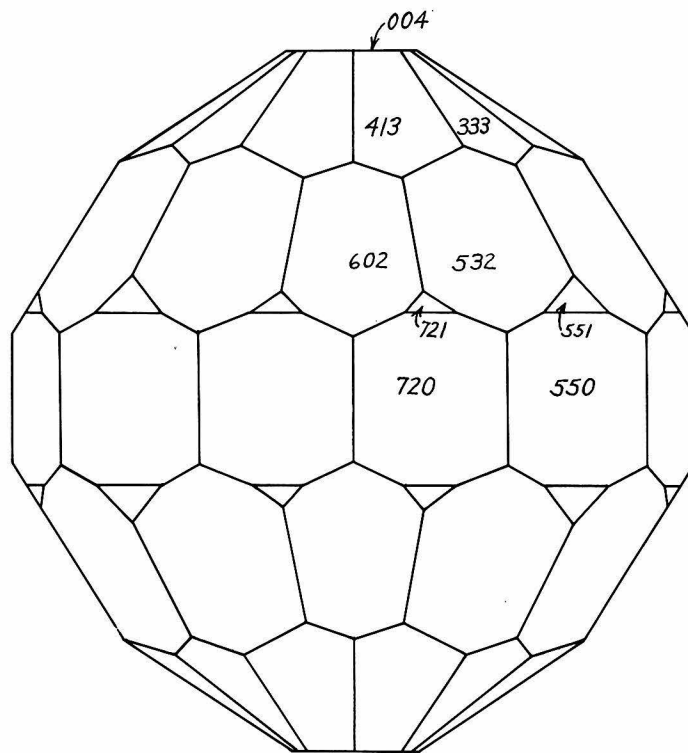


Figure 10. The polyhedron of the second strong Brillouin zone in  $\sigma$ -FeCr (courtesy Dr. Shoemaker).

represents approximately the minimum iron content in this sigma phase; the maximum iron content is variously reported to be 56<sup>(1)</sup> to 58<sup>(26)</sup> at. %. Hence over the entire range of composition of  $\sigma$ -FeCr the average number of electrons per atom exceeds the number accommodated by the observed strong polyhedron. If it is assumed that the Brillouin zone should be filled, the excess of electrons over an average of 6.97 per atom should go into non-binding orbitals, presumably 3d, perhaps giving rise to ferromagnetism (which does not seem to exist in the sigma phase) or anti-ferromagnetism. For a sigma FeCr phase with 58 at. % iron, the average number of electrons per atom is 7.16, or about 0.2 electrons per atom in excess of the number provided for in the filled zone. The sigma phase occurs in the FeV-system with ~~as much as~~ 43 to 63 at. % iron<sup>(26)</sup>. Vanadium has only five valence electrons as compared to six for chromium, and hence the average number of electrons per atom varies from 6.29 to 6.89; even the maximum number is insufficient to fill the zone completely. The  $\delta$ -phase in the CoCr-system<sup>(27)</sup>, which is probably the sigma phase, exists with a cobalt content ranging from about 34 to about 43 at. % cobalt. For the minimum cobalt content there are 7.02 electrons per atom, and for the maximum cobalt content there are 7.29, so that as in  $\sigma$ -FeCr there is an excess over 6.97 over the entire range. Although the composition ranges for all of these phases provide in the neighborhood of seven electrons per atom, there seems to be no clear-cut indication that the composition limits are determined by the Brillouin polyhedron. Therefore it appears to be possible that the actual

valences are of the order of magnitude of those already given in Table VIII, and that the Brillouin polyhedron is in all cases unfilled.

#### WORK ON THE IRON-MOLYBDENUM SIGMA PHASE STRUCTURE

Introduction - As has been stated earlier it was not possible to draw perfectly reliable conclusions as to the ordering of the iron and chromium atoms in the sigma structure from the x-ray diffraction data as the difference between the form factors for iron and chromium is too small. Therefore it became a matter of great interest to try to determine the ordering of the atoms in some other binary sigma phase in which the two atoms have considerably different form factors and consequently x-ray data could be expected to give the necessary information. When we learned that Professor Duwez and Mr. Paul Pietrokovsky had found the sigma structure also in the iron-molybdenum system we became very interested in trying to determine the ordering of the atoms in this phase. Professor Duwez kindly furnished us with a powder sample of a FeMo sigma structure.

Materials - The sample had been prepared as follows. Iron and molybdenum powders (325-mesh) were mixed in the atomic proportions 1:1 and then compressed to a pellet under a pressure of 72,500 lb/sq in. The pellet was then heated to 2600° F. and kept at this temperature for four hours, after which it was crushed. The coarse powder was

annealed for ten minutes at 2600° F. and then quenched in a stream of helium gas in order to "freeze in" the sigma phase, which is apparently unstable at lower temperatures.

Single crystal work - By the same method that was applied in the work on the  $\sigma$ -FeCr, a single crystal of the FeMo sigma phase was found in the sample furnished by Professor Duwez. It was considerably more difficult to find a single crystal in this case as the powder particles in general appeared to be built up from very small crystallites. The single crystal that finally was found was less than 0.01 mm in diameter. With this crystal Laue photographs were obtained that confirmed the tetragonal symmetry of the structure. Photographs were taken with the beam parallel to the  $a$ -axis and the  $c$ -axis. Attempts were then made to collect intensity data by Weissenberg photography. Although this no doubt is possible even with the very small crystal used here the work was interrupted as it turned out that exposures of more than 500 hours were required for reasonably good photographs. At the time this thesis is written the search for larger single crystals is in progress.

Powder work - In order to obtain data for the determination of the cell constants of the FeMo sigma structure some powder photographs were also taken. The photographs showed exactly the same general type of pattern as the photographs obtained with the FeCr samples, and since the symmetry of the FeMo structure had been found to be tetragonal it could be concluded that the two structures are the



same, except possibly with respect to ordering. The photographs have not yet been measured accurately. A preliminary determination of the cell constants has been made, however, based on the data obtained from seven easily measurable lines, with the following results:

$$a_0 = 9.188 \pm 0.002 \text{ \AA}$$

$$c_0 = 4.812 \pm 0.002 \text{ \AA}$$

Discussion - The values found for  $a_0$  and  $c_0$  are respectively 4.5% and 5.8% larger than the corresponding values found for  $\sigma$ -FeCr. The fact that the value of  $c_0$  has increased more than the value of  $a_0$  may be interpreted as indicating that the atoms E are molybdenum as these atoms very likely have more influence on the value of  $c_0$  due to the very short E-E bonds. It will be recalled that in the previous discussion of ordering the  $\sigma$ -FeCr structure, all three considerations led to the prediction that atoms E are predominantly chromium; this is consistent with the interpretation just made in the FeMo-structure.

This is as far as the work on the iron-molybdenum sigma structure has progressed at the time this thesis is written. We hope that it will be possible to find larger single crystals which would greatly facilitate the collection of intensity data. If larger single crystals cannot be found it will nevertheless probably be possible to get the necessary intensity data either with the crystal found so far or from powder photographs.

SUMMARY

The crystal structure of the sigma phase in the iron-chromium system at 46.5 at.-% chromium content has been determined by the application of x-ray diffraction methods. The crystal lattice was found to be primitive tetragonal with the following dimensions for the unit cell:

$$a_0 = 8.7995 \pm 0.0004 \text{ \AA.} \quad c_0 = 4.5442 \pm 0.0020 \text{ \AA.}$$

The space group is almost certainly  $D_{4h}^{14}$ -P4/mnm. The thirty atoms in the unit cell are in the following positions:

Atoms A in 2(a)

Atoms B in 4(f) with  $x = 0.3981 \pm 0.0006$

Atoms C in 8(i) with  $x = 0.4632 \pm 0.0007$ ;  $y = 0.1316 \pm 0.0006$

Atoms D in 8(i) with  $x = 0.7376 \pm 0.0006$ ;  $y = 0.0653 \pm 0.0006$

Atoms E in 8(j) with  $x = 0.1823 \pm 0.0006$ ;  $z = 0.2524 \pm 0.0006$

The kind and degree of ordering of the iron and chromium atoms could not be determined.

The structure is conveniently described as being built up from atoms situated at the net points of two pseudo-hexagonal nets, one on top of the other and oriented at  $90^\circ$  to each other. Eight of the thirty atoms in the unit cell are displaced so that they are about half-way between two pseudo-hexagonal layers. The observed hardness and brittleness of the sigma phase can be explained by the fact that the possibility of slip is very much reduced by the locking action of the displaced atoms.

The iron-molybdenum sigma phase has also been studied to a limited extent. That the structure of the phase is of the same type as the iron-chromium sigma structure was confirmed by comparing Laue photographs and powder photographs of  $\sigma$ -FeMo with corresponding photographs of  $\sigma$ -FeCr. The unit cell of  $\sigma$ -FeMo was found to be slightly larger than that of  $\sigma$ -FeCr. The cell dimensions were found to be

$$a_0 = 9.188 \pm 0.002 \text{ \AA} \quad c_0 = 4.812 \pm 0.002 \text{ \AA}.$$

The kind and degree of ordering of the iron and molybdenum atoms have not yet been investigated but there is good reason to believe that it can be found quite easily from x-ray diffraction data.

ACKNOWLEDGEMENTS

I have previously acknowledged the very valuable contributions made by Professor Linus Pauling and Dr. David Shoemaker. I am particularly indebted to Dr. Shoemaker for making available for the preparation of this thesis three drawings that had been made earlier for other purposes. I am also indebted to him for having suggested many revisions and interpretations.

I am very much indebted to Professor Pol Duwez and Mr. Paul Pietrokowsky for furnishing the sigma phase samples, for making powder photographs available and for suggestions and valuable discussions.

I am indebted to Professor J. H. Sturdivant and Professor Verner Schomaker for valuable suggestions and discussions.

I want to express my thanks to Mrs. Nan Arp for carrying out a great number of calculations.

I also want to acknowledge the financial aid given to me by the Ethyl Corporation in form of a fellowship for the academic year 1950-51.

This work was done in part under a contract with the Office of Naval Research and in part under a program sponsored by the Carbide and Carbon Chemicals Corporation.

REFERENCES

1. Metals Handbook, American Society for Metals, Cleveland, 1948 Edition, p. 1194.
2. E. C. Bain and W. E. Griffiths, Trans. AIME, 75, 166 (1927).
3. P. Duwez and S. R. Baen, X-Ray Study of the Sigma Phase in Various Alloy Systems, A.S.T.M. Preprint, 47, (1950).
4. A. J. Bradley and H. J. Goldschmidt, J. Iron Steel Inst., 11, 273-288 (1941).
5. F. Wever and W. Jellinghaus, Mitt. K. W. Inst. Eisenforschung, 12, 317-322 (1930).
6. A. R. Elsea, A. W. Westerman and G. K. Manning, Trans AIME, Tech. Paper No. 2393, (June, 1948).
7. P. A. Beck and W. D. Manly, Journal of Metals, 1, 354 (1949).
8. H. J. Goldschmidt, Research 2, 343-344 (1949).
9. P. Duwez and P. Pietrokovsky, unpublished.
10. This thesis, p. 88.
11. A. J. Bradley and H. J. Goldschmidt, J. Iron Steel Inst., 144, 273 (1941).
12. P. Pietrokovsky, unpublished work.
13. J. J. de Lange, J. M. Robertson, and I. Woodward, Proc. Roy. Soc., A171, 398 (1939).
14. Internationale Tabellen zur Bestimmung von Kristallstrukturen, Gebruder Borntraeger, Berlin, 1935. Band I, page 221.
15. D. P. Shoemaker and B. G. Bergman, J. Am. Chem. Soc., 72, 5793 (1950).
16. G. J. Dickins, A. M. B. Douglas, and W. H. Taylor, J. Iron Steel Inst., 167, 27 (1951) and Nature, 167, 192 (1951).
17. C. W. Tucker, Jr., Science, 112, 448 (1950); Report AECD-2957, entitled "An Approximate Crystal Structure for the Beta Phase of Uranium", Knolls Atomic Power Laboratory, Schenectady, July 7, 1950.

REFERENCES (continued)

18. B. G. Bergman and D. P. Shoemaker, J. Chem. Phys., 19, 515 (1951).
19. D. P. Shoemaker, Doctoral Dissertation, California Institute of Technology, 1947.
20. H. E. Seeman, Eastman Kodak Company, private communication to D. P. Shoemaker, 1947.
21. E. W. Hughes, J. Am. Chem. Soc., 63, 1838 (1941).
22. L. Pauling, J. Am. Chem. Soc., 69, 542 (1947).
23. L. Pauling, Proc. Roy. Soc. A, 196, 343 (1949).
24. L. Pauling and F. J. Ewing, Rev. Mod. Phys. 20, 112 (1948).
25. H. Kuhn, J. Chem. Phys., 16, 727 (1948).
26. P. Pietrokovsky, private conversation.
27. M. Hansen, Der Aufbau der Zweistofflegierungen, Julius Springer, Berlin, 1936, p. 481.

PROPOSITIONS

1. The determination of the crystal structures of many substances, e.g. intermetallic compounds, is often considered possible only by the application of the powder method as the substances are usually obtained in a microcrystalline state. Based on experience on the sigma phase in the FeCr and FeMo systems<sup>(1)</sup> I believe that in many such cases single crystal work can be done with specimens isolated from a coarsely-ground sample with use of a microscope. Indications as to whether this method can be considered promising in an individual case can be obtained by observing the degree of graininess of powder lines in powder photographs taken of the coarsely-ground sample.
2. The often very difficult task of indexing the lines on powder photographs would be considerably easier if the degeneracy of the lines were known. It should be possible to determine the degeneracy in many cases from the density of grains in the powder lines on a photograph taken of a coarsely-ground sample.
3. The degree and kind of ordering of the iron and molybdenum atoms in the iron-molybdenum sigma phase can very likely be determined by ordinary x-ray diffraction methods as the form factors of the two metals differ considerably. This is however not the case for the iron-chromium sigma phase in which the form factors are about the same with copper radiation. It is reasonable to assume that the ordering may be the same in some respects in this phase as in the iron-molybdenum phase, but, of course, the difference in atomic radius ratio may cause some differences in ordering. Direct information is very desirable in the case of the FeCr-phase. I therefore propose that new intensity data be obtained with sigma FeCr crystals using Mn K $\alpha$  radiation. Due to anomalous dispersion it can be expected that the atomic form factors for zero scattering angle would be about 24 for iron and 20 or less for chromium i.e. a difference of four or more instead of the normal two. This greater difference should suffice for at least an approximate determination of the ordering of the atoms in the structure.
4. Köster and Tonn<sup>(2)</sup> have investigated the phase diagrams of the CoW and CoMo systems. The two phase diagrams have the same general features. Compounds of the approximate composition CoW and CoMo respectively were found to exist within a rather narrow range of composition. Sykes and Graff<sup>(3)</sup> have reinvestigated the CoMo system with essentially the same results as Köster and Tonn obtained. They also observed a compound of the approximate composition CoMo which they found

to be most easily identified by its characteristic powder pattern with the most distinguishable lines corresponding to the interplanar distances 2.34 Å, 2.14 Å, 2.10 Å, 2.06 Å and 2.007 Å. The most distinguishable lines in FeMo sigma powder pattern correspond to the interplanar distances 2.41 Å, 2.23 Å, 2.17 Å, 2.13 Å, 2.07 Å, 2.02 Å and 1.98 Å. I therefore propose that the CoW and CoMo compounds be reinvestigated by the powder method in order to determine whether or not they have the sigma structure.

5. I have found that when illuminating gas is mixed with the vapor of silicon tetrachloride and burned with enough air to give a hot flame, a smoke of silicon dioxide is formed that consists of extremely small particles, so small in fact that the smoke is barely visible and has a blueish color. If the flame is allowed to impinge on some solid object the smoke is precipitated as a translucent solid having much the appearance of a gel and having an extremely low density (as low as 0.03 of the density of silicon dioxide). Nevertheless it has a surprising mechanical strength. In layers having thicknesses of several millimeters it transmits light with a yellowish color while the light scattered by the substance at 90° is bluish and almost completely polarized, indicating that the particles of which the substance is built up are very small.

I propose

(a) That this substance be investigated with the x-ray powder method in order to determine the approximate particle size from the broadness of the powder lines, and

(b) that in view of the considerable mechanical strength of this substance and its highly porous nature its suitability as a material for membranes for gaseous diffusion be investigated.

6. In distillation columns the repeated exchange of material between the liquid and gaseous phase takes place either on the "plates" or on the surface of the small bodies with which the column is filled. It may be expected that a very good exchange should also be achieved for a small drop of liquid of appropriate size falling freely through the vapor. I propose that the functioning of a distillation column be investigated that consists of an empty column, at the top of which the reflux liquid is sprayed down with the drop size as uniform as possible.

7. In his book "The Optical Principles of the Diffraction of X-Rays", R. W. James<sup>(4)</sup> claims that the formula for the total intensity of the x-rays scattered by a molecular liquid, first derived by Menke, can be applied without regard to the partial ordering of adjacent molecules. This does not seem to be correct.



8. Dr. Adam Schuch<sup>(5)</sup> has observed that metallic cerium subject to stresses goes over into another modification that also has the cubic close packed structure but a smaller unit cell. He gives the possible explanation that the 4f electron has moved up into a hybridized 5d5s orbital where it is able to participate in the metallic bonding. The increase in energy in this change cannot be very large.

I propose that the electric resistivity and magnetic susceptibility be determined for paramagnetic cerium compounds like CeS at different temperatures as it is possible that thermal excitation could cause the 4f to 5d5s transition to take place to some extent.

9. For the intermetallic compound CeAl<sub>2</sub>, which has the MgCu<sub>2</sub> structure and is remarkable for having a very high melting point, the valences calculated for aluminum and cerium from the interatomic distances in the usual way are found to be 2.7 and 4.4. In view of the nature of such compounds as AuAl<sub>2</sub> (fluorite structure), for which there is a good case for electron transfer, it would seem likely that electron transfer takes place in CeAl<sub>2</sub> (and LaAl<sub>2</sub>, etc.) from cerium to aluminum, the 4d electrons of cerium presumably being used. However, for the compound CaAl<sub>2</sub>, which has the same structure as CeAl<sub>2</sub> and also has a high melting point, it is hard to see how increase of total valences by electron transfer can take place, although the valences of calcium and aluminum are calculated in the usual way to be 7.3 and 3.3 respectively. Hence it appears that other phenomena than electron transfer must be considered in explaining the extraordinary stability of compounds of this type.

10. For the two intermetallic compounds CoAl and NiAl, both of which have the cesium chloride structure and are remarkable for their very high melting points, the valences calculated from the observed interatomic distances in the usual way are 7.2 for aluminum and 7.9 for cobalt and nickel. The actual valences cannot of course be that high, but it would appear that all of the electrons beyond the argon shell in nickel and cobalt are used in bonding. It would therefore be of interest to investigate the magnetic susceptibilities of these compounds.

11. The name Ångström is almost universally mispronounced in English speaking countries. I therefore propose that when the name is written in full in these countries it be spelled Åwngstrum, with symbol Åw.

REFERENCES

1. B. G. Bergman, Thesis, California Institute of Technology (1951).
2. W. Köster and W. Tonn, Z. f. Metallkunde, 24, 296 (1932).
3. W. P. Sykes and H. F. Graff, Trans ASM, 23, 249 (1935).
4. R. W. James, The Optical Principles of the Diffraction of X-Rays, p. 496, G. Bell & Sons, Ltd., London (1950).
5. A. Schuch, Thesis, California Institute of Technology (1950).